Late Mesozoic compressional to extensional tectonics in the Yiwulüshan massif, NE China and its bearing on the evolution of the Yinshan-Yanshan orogenic belt: Part I: Structural analyses and geochronological constraints

Wei Lin, Michel Faure, Yan Chen, Wenbin Ji, Fei Wang, Lin Wu, Nicolas Charles, Jun Wang, Qingchen Wang

Late Mesozoic compressional to extensional tectonics in the Yiwulüshan massif, NE China and its bearing on the evolution of the Yinshan–Yanshan orogenic belt: Part I: Structural analyses and geochronological constraints

- Wei Lin[a]
- Michel Faure[b]
- Yan Chen[b]
- Wenbin Ji[a]
- Fei Wang[a]
- Lin Wu[a]
- Nicolas Charles[b]
- Jun Wang[a]
- Qingchen Wang[a]

- [a] State Key Laboratory of Lithospheric Evolution, Institute of Geology and Geophysics, Chinese Academy of Sciences, P.O. Box 9825, Beijing 100029, China
- [b] Institut des Sciences de la Terre d'Orléans, UMR6113, Université d'Orléans-INSU/CNRS, 1A rue de la Férollerie, 45071 Orléans, France

Abstract

With a cratonic nucleus, the North China Craton (NCC) experienced a complex tectonic evolution with multiphase compressional and extensional events during Mesozoic times. Along the northern part of the NCC, the Yinshan–Yanshan fold and thrust belt was a typical intraplate orogen. Jurassic and Cretaceous continental sedimentation, magmatism, widespread intraplate characterize the Yinshan–Yanshan orogenic belt. The geodynamic significance of these tectonic events is still in dispute. In the western part of the Liaoning province, the Yiwulüshan massif crops out at the eastern end of the Yinshan–Yanshan orogenic belt. The Yiwulüshan massif presents an elliptical domal shape with a NE–SW striking long axis. The structural evolution of this massif brings new insights for the understanding of the Mesozoic plutonic–tectonic history of the NCC. A multidisciplinary study involving structural geology, geochronology, Anisotropy of Magnetic Susceptibility (AMS) and gravity modeling have been carried out. The presentation of the new results splits into two parts. Part I (this paper) deals with field and laboratory structural observations, and presents the main geochronological results. The AMS, gravity modeling data will be provided in a companion paper (Part II). The early compressional deformation (D_1) corresponds to a Late Jurassic to Early Cretaceous southward thrusting. The subsequent deformation is related to the Early Cretaceous exhumation of the Yiwulüshan massif. A detailed structural analysis allows us to distinguish several deformation events (D_2, D_3, and D_4). The Cretaceous extensional structures, such as syntectonic plutons bounded by ductile normal faults, metamorphic core complexes, and half-graben basins are recognized in many places in East Asia. These new data from the Yiwulüshan massif constitute a link between Transbaikalia, Mongolia, North China and South China, indicating that NW–SE extensional Mesozoic tectonics occurred throughout the entire region.

Highlights

► Structural geology and geochronology improve the knowledge of the NCC destruction. ► The Yiwulüshan massif is an example of deformation from compression to extension. ► New data link extensional tectonics of North China, Transbaikalia, and South China.

Keywords

- North China Craton;
- Yinshan–Yanshan fold and thrust belt;
- Yiwulüshan massif;
- Structural analysis;
- Polyphase deformations

1. Introduction

After its Neoarchean to Proterozoic evolution ([Zhao et al., 2003], [Faure et al., 2007], [Trap et al., 2007] and [Zhai and Santosh, 2011]), the North China Craton (NCC) experienced a complex tectonic evolution during Late Paleozoic–Mesozoic times (e.g. [Yin and Nie, 1993], [Yin and Nie, 1996], [Davis et al., 2001], [Kusky and Li, 2003] and [Kusky, 2011]). The Qinling–Dabie belt is the boundary between the NCC and South China Blocks (SCB). The presence of UHP metamorphic rocks attest to a very deep subduction of the continental crust of the SCB below the NCC (e.g., [Mattauer et al., 1985], [Yin and Nie, 1993], [Faure et al., 1999], [Faure et al., 2003], [Ratschbacher et al., 2003], [Hacker et al., 2006] and [Hacker et al., 2009] and references therein). To the north, the Solonker suture zone (Fig. 1) corresponds to the collision zone between the NCC and the Paleozoic Mongolian magmatic arcs ([Sengor and Natal'in, 1996], [Xiao et al., 2003] and [Chen et al., 2008] and references therein). The age of the collision remains debated, from Early Paleozoic to Early Triassic times ([Wang and Liu, 1986], [Xu and Chen, 1997], [Xiao et al., 2003] and [Shang, 2004]). Whatever the geodynamic models, it is well acknowledged that the amalgamation of the NCC with neighboring blocks was completed in Late Triassic. These two collisional events were followed by a localized Jurassic to Early Cretaceous compressional deformation ([Davis et al., 1996] and [Davis et al., 2001]) and widespread Early Cretaceous to Eocene extensional structures are responsible for lithospheric thinning ([Zhai et al., 2004], [Lin and Wang, 2006] and [Li et al., 2011a]). Unlike most of Precambrian cratons that have thick sub-continental mantle lithospheric roots, the mantle lithosphere beneath the NCC is considered to be less than 80 km owing to these tectonic events. The old and thick Archean mantle lithosphere beneath the NCC is believed to have been replaced by juvenile lithospheric mantle (Wu et al., 2008 and reference therein; Yang and Wu, 2009). The processes and mechanisms of the destruction of the NCC have become a topic of interest in Earth sciences worldwide (Carlson et al., 2005).

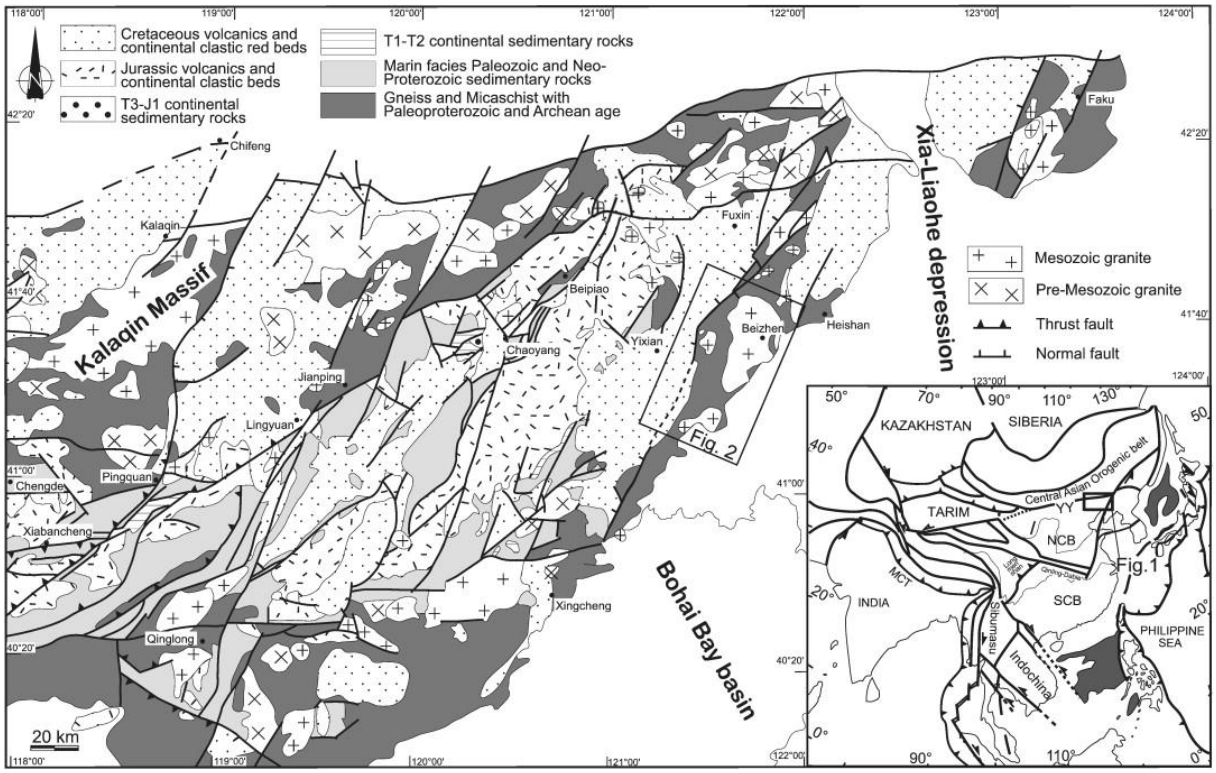

Fig. 1. Simplified geological map of the eastern Yinshan–Yanshan belt and the location of the Yiwulüshan massif (modified from Du et al., 2007).

In the northern part of the NCC, the Yinshan–Yanshan fold and thrust belt (or Yinshan–Yanshan belt) is a typical intraplate orogen that extend east–west, at about 40°N latitude, from west of the Tan-Lu fault and western Liaoning province to the western Inner Mongolia along more than 1000 km (Fig. 1). Jurassic coal-bearing clastics and continental volcano-sedimentary units unconformably overlay the older units ranging in age from Archean to Triassic (HBGMR, 1989). The geology of the Yinshan–Yanshan belt (Fig. 1) has attracted the attention of Chinese geologists for about one century (e.g. Wong, 1929). The Jurassic–Cretaceous "Yanshanian" Orogeny was named after this region and, subsequently, applied to all the Jurassic–Cretaceous tectonic events throughout China. The Yinshan–Yanshan belt is characterized by Jurassic and Cretaceous continental sedimentation, magmatism, and widespread intracontinental tectonics with several compressional, extensional, and strike-slip deformation phases ([Davis et al., 1998] and [Davis et al., 2001]). The origin of the Yanshan–Yinshan belt was variously interpreted to be related to i) the collision between Siberia and Mongolia after the closure of the Mongol–Okhotsk Ocean (Yin and Nie, 1996), ii) the subduction of the Paleopacific plate beneath Eastern Eurasia ([Xu and Wang, 1983], [Zhu et al., 2011a] and [Zhu et al., 2011b]), iii) the interactions of north–south Eurasian intraplate deformation and northwestward Pacific Ocean subduction and attendant arc magmatism (Davis et al., 2001) or iv) formed independently of plate interactions in Eastern Asia (e.g. Cui and Wu, 1997). A multidisciplinary study has been carried out in the Yiwulüshan massif, which is a typical area of the Yinshan–Yanshan fold and thrust belt that recorded Mesozoic polyphase deformation events. Several approaches have been applied, such as structural geology, $^{40}Ar/^{39}Ar$ geochronology on different potassium rich minerals, U–Pb geochronology on zircon, Anisotropy of Magnetic Susceptibility (AMS) on granite massif and gravity modeling on granite. The AMS and gravity data will be presented in the companion paper (Lin et al., this issue).

2. Geological overview of Yiwulüshan massif as the witness of Late Mesozoic compression and extension in the Yinshan–Yanshan belt

In the eastern end of the Yinshan–Yanshan belt, the Yiwulüshan massif (Fig. 1) is a typical region that illustrates the tectonic evolution of the Yinshan–Yanshan belt. The Yiwulüshan massif is bounded to the east by the NNE-trending Cretaceous to Eocene Xia–Liaohe depression, the northern part of the Bohai Bay basin, and to the west by the Fuxin–Yixian Cretaceous graben (Fig. 1 and Fig. 2; Li et al., 2011b). The Yiwulüshan massif can be divided into three main litho-tectonic units which are, from bottom to top: 1) an orthogneissic monzogranitic unit of Neoarchean or Paleoproterozoic metamorphic rocks considered to represent the basement rocks of the Yinshan–Yanshan belt ([LBGMR, Liaoning Bureau of Geology and Mineral Resources, 1989], [Ma et al., 1999] and [Zhang et al., 2002]); 2) a plagioclase–amphibolite and micaschist unit of Paleoproterozoic age ([LNBGMR-Yixian, 1970] and [LBGMR, Liaoning Bureau of Geology and Mineral Resources, 1989]); and 3) a Mesoproterozoic to Mesozoic sedimentary cover ([LNBGMR-Yixian, 1970], [Ma et al., 1999], [Ma et al., 2000] and [Zhu et al., 2003]). These three units are intruded by several generations of Mesozoic plutons.

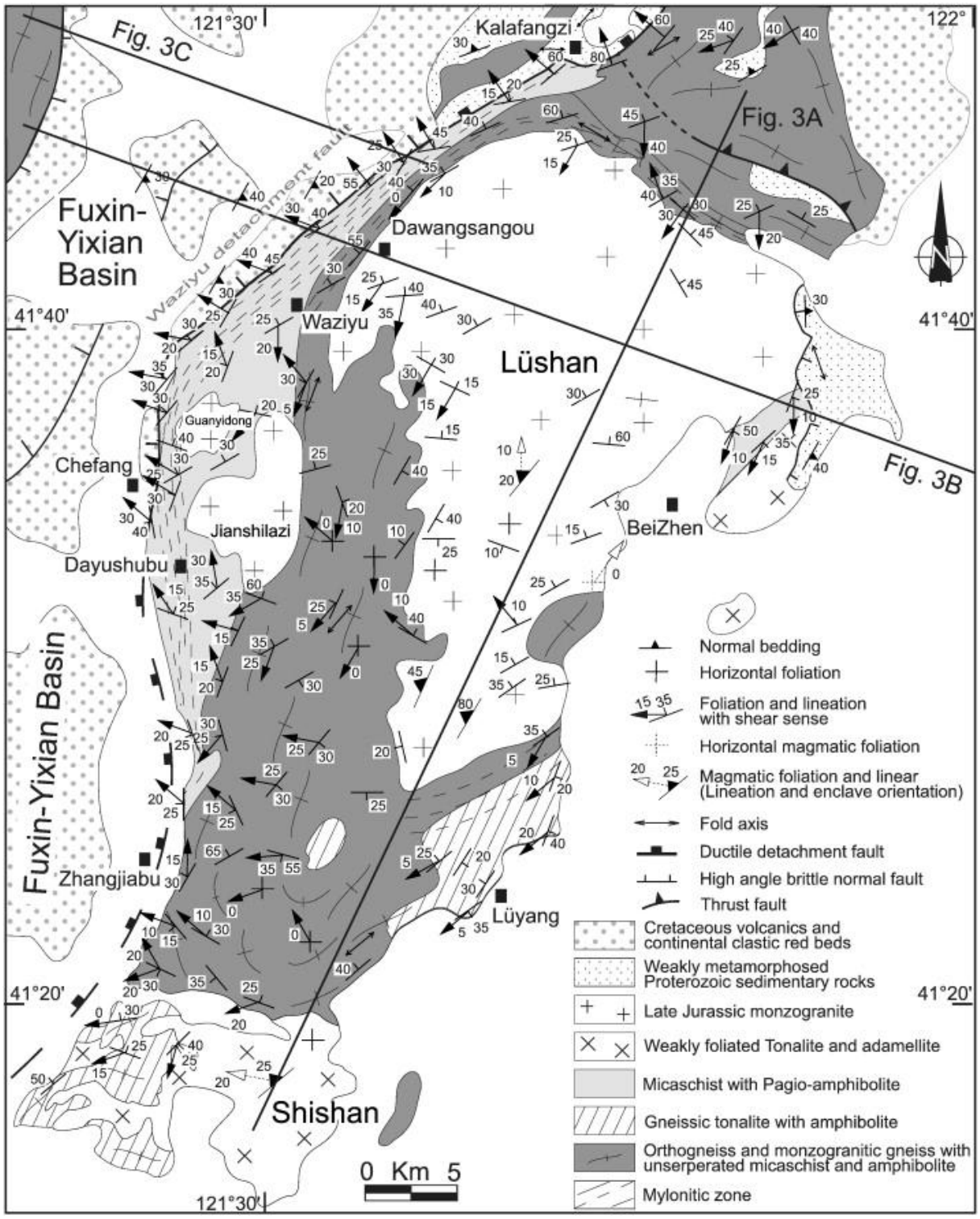

Fig. 2. Structural map of the Yiwulüshan massif.

Located near the Beizhen city, the Yiwulüshan massif presents an elliptical shape of ca 60×30 km^2 with a NNE–SSW oriented long axis (Fig. 2). According to previous studies and our own field work, the Yiwulüshan massif essentially exposes metamorphic and granitic rocks ([Ma et al., 1999], [Ma et al., 2000] and [Darby et al., 2004]). The Jurassic plutons intrude into the metamorphic rocks (Fig. 2). The basement rocks can be separated into two parts: gray to black and gray to white porphyritic orthogneiss, and metasedimentary rocks

with amphibolite, plagioclase–amphibolite, micaschist, and magnetite quartzite. Most of the sedimentary rocks belong to Mesoproterozoic to Mesozoic series (LBGMR, Liaoning Bureau of Geology and Mineral Resources, 1989; Fig. 2). In the eastern and northern parts of the massif, Mesoproterozoic to Neoproterozoic (Changcheng to Wumishan Groups) rocks consist of carbonates (limestone, dolomite and marble), sandstones, and quartzites (LNBGMR-Yixian, 1970). The Paleozoic series does not crop out in the research area, but more to the west, near the Fuxin–Yixian basin, the Paleozoic series can be observed, except for the Late Ordovician to Middle Carboniferous formations (Fig. 1).

The Mesozoic strata are well defined from a large opencast coal mine in the Fuxin–Yixian basin, which is situated to the north of the research area. From bottom to top, the "Yixian Formation" is mostly formed by volcanic rocks of mafic, intermediate-felsic, and felsic compositions, and several intercalated sedimentary layers. The ages of the volcanic rocks range from 135 to 120 Ma ([LBGMR, Liaoning Bureau of Geology and Mineral Resources, 1989] and [Peng et al., 2003]). The "Jiufotang Formation" consists of shale and siltstone deposited in deep lacustrine sedimentary environment (Wang et al., 1998b). The upper part of the series is represented by the "Shahai Formation" sandstone and siltstone of deep to shallow water lacustrine sedimentation ([LBGMR, Liaoning Bureau of Geology and Mineral Resources, 1989] and [Li, 1994]).

Mesozoic granitoid plutons occupy most part of the massif (Fig. 2). On the basis of petrological and geochronological studies, two groups of plutonic rocks can be distinguished in the study area. The Lüshan pluton, situated in the central part of the massif, is the largest Mesozoic pluton in the western Liaoning province. It is composed of medium to fine-grained gray-colored monzogranite and granodiorite. Plagioclase, K-feldspar, amphibole, biotite and muscovite are the dominant minerals; garnet occurs as accessory phase (LBGMR, 1989). The geochronological studies from the Lüshan pluton reveal a large time span: the method of SHRIMP U/Pb and ICP-MS have been carried on zircon, the former yields late Jurassic ages of 162.8 ~ 153.5 Ma; while the latter yield ages of 153 ± 2 Ma, 163 ± 3 Ma, and 152.6 ± 1.8 Ma ([Wu et al., 2006], [Yin, 2007] and [Zhang et al., 2008]). On the west of the pluton, the granitic rocks are deformed and even mylonitized. The mylonitization is well developed along the western margin of pluton and decreases towards the center. But, in fact, the deformation is not homogeneous, several centimeters scale mylonitic zones have been observed inside the pluton. Lying to the western part of the massif, the Jianshilazi and Guanyindong plutons are entirely composed of biotite bearing monzogranite and granodiorite. Geochronology indicates similar intrusion ages as for the Lüshan pluton ([Darby et al., 2004] and [Wu et al., 2006]). In the south and east of the Yiwulüshan massif, a medium to fine-grained tonalite and adamellite Shishan pluton crops out (Fig. 2). However, according to recent ICP-MS zircon U–Pb age of 123.0 ± 3.0 Ma, this pluton must be considered as an early Cretaceous intrusion (Wu et al., 2006).

In the Yiwulüshan massif, deformation features were considered by previous workers to have been formed in a variety of tectonic settings: 1) On the basis of the ductile shear zone observed along the western side of the massif, which was considered to extend for more than 150 km (LBGMR, 1989), a "Yanshanian" (Jurassic to Cretaceous) or "Indosinian" (Late Triassic) metamorphic core complex (MCC) has been suggested (Lü and Liu, 1994). 2) According to the understanding of the geometry and the deformation, [Ma et al., 1999] and [Ma et al., 2000] and Zhu et al. (2003) considered that the Yiwulüshan massif was a "Yanshanian" MCC, as suggested, by the detachment fault situated along the western margin of the massif. But they proposed a "symmetric" MCC structure. 3) After their

$^{40}Ar/^{39}Ar$ dating of the ductile shear zones situated to the northern and northwestern parts of the massif, Zhang et al. (2002) distinguished two stages of ductile deformation: namely, an early, dextral one with a late Triassic age (219 ± 4 Ma) and a Cretaceous extensional and sinistral strike-slip one characterized by $^{40}Ar/^{39}Ar$ ages comprised between 116 ± 2 Ma and 127 ± 3 Ma, and superimposed on the late Triassic shear zone. 4) Concentrating on the regional Jurassic compressional deformation, Zhang et al. (2004) interpreted the NE–SW structures along the western margin of Yiwulüshan massif as due to a sinistral strike-slip related to a Jurassic thrust. 5). On the basis of the structural analysis, especially the kinematics along WNW–ESE mineral and stretching lineation, Darby et al. (2004) emphasized the NE–SW striking structures along the western margin of the Yiwulüshan massif, as the Waziyu detachment fault, and renamed the Yiwulüshan MCC as the Waziyu MCC. The top-to-the-W, or WNW, shearing and its geochronological age around 127–116 Ma was first mentioned by Darby et al. (2004). 6) On the basis of geochemistry, Liu et al. (2000) interpreted the Lüshan monzogranite as a syntectonic granite emplaced in an extensional tectonic setting.

3. Structural analysis in the Yiwulüshan massif

3.1. Lithological units and bulk architecture of the Yiwulüshan massif

The Yiwulüshan massif is a metamorphic NE–SW trending structure bounded by Mesozoic and Cenozoic basins, the Fuxin–Yixian basin and the Xia–Liaohe Depression to the west and to the east, respectively (Fig. 2). The Fuxin–Yixian Basin is filled by various continental sedimentary rocks alternating with unmetamorphosed basaltic and andesitic lava flows. According to paleontological data and lithological correlations, these rocks are likely late Jurassic to early Cretaceous age ([LBGMR, Liaoning Bureau of Geology and Mineral Resources, 1989] and [Zhang et al., 2005]).

The bulk architecture of the Yiwulüshan massif is dominated by a NE–SW elongated dome, which results from a polyphase evolution (Fig. 2 and Fig. 3). The heterogeneously deformed monzogranite forms the core of the dome. In the central part, the major part of the pluton is not or weakly foliated. In some place, magmatic foliations can be observed (Fig. 2 and Fig. 4A). Our field work indicates that the mafic enclaves and K-feldspar megacrysts exhibit a preferred NE–SW orientation (Fig. 5B). Centimeter-thick mylonitic zones can be observed in several places (Figs. 4B, 5A). In the pluton margins, especially on the Northern and Western parts, the deformation is relatively strong as suggested by the conspicuous development of the foliation (Fig. 2 and Fig. 3A,B). Wherever the places are in the massif, the post-solidus foliation in the Lüshan, Jianshilazi and Guanyidong plutons exhibits a relatively low dip (Fig. 5A). Near the boundary between the granite and country rocks, for example at Dawansangou, in the NW of the massif, centimeter scale oriented xenoliths of orthogneiss and amphibolite exhibit foliations both parallel to the granite-host rock contact and the foliation in the country rocks (Fig. 2).

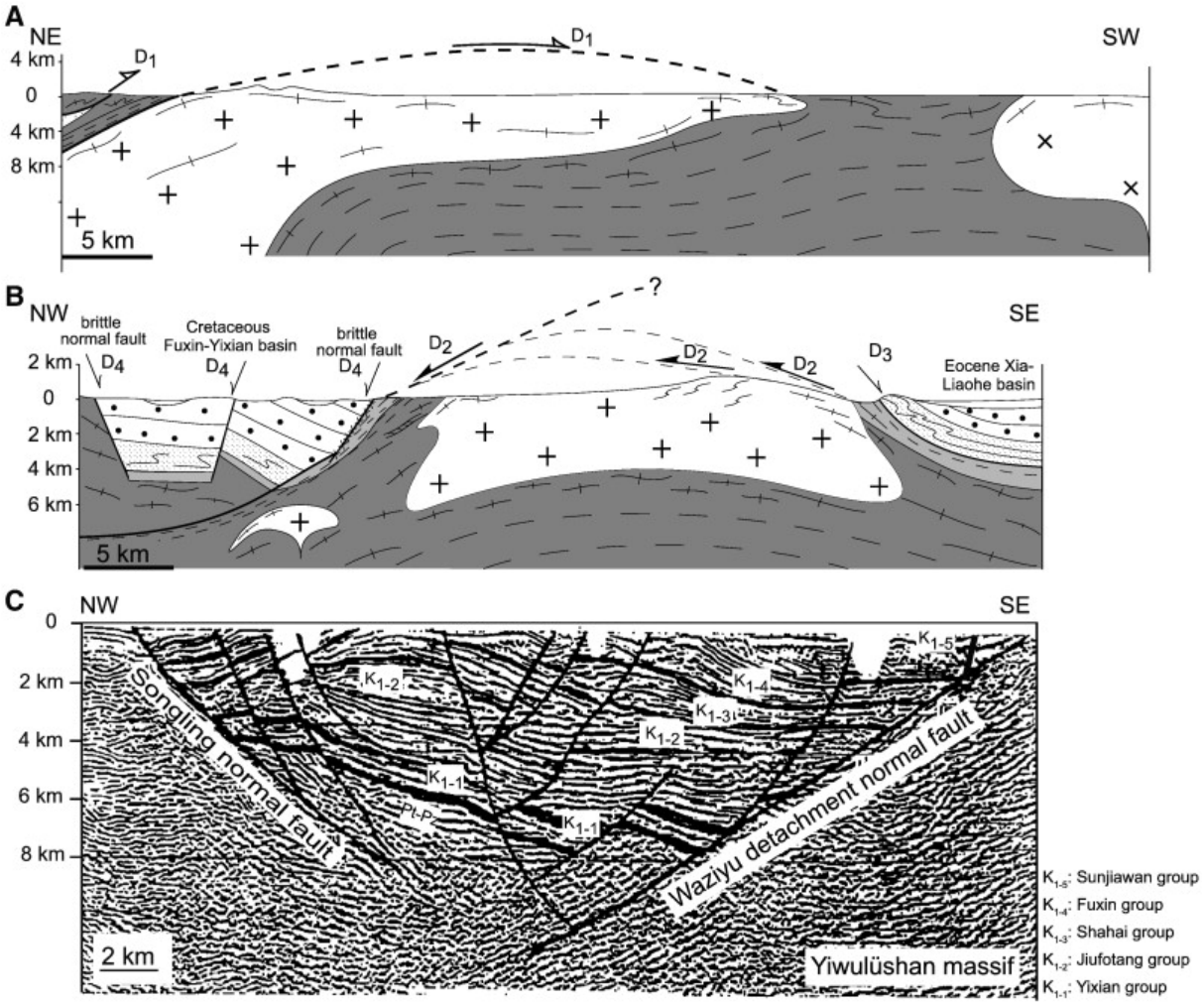

Fig. 3. Cross-sections though the Yiwulüshan massif and Fuxin–Yixian basin (the pluton roots are hypothetic. Location in Fig. 2 and figure captions are the same as in Fig. 2). A: Cross-section drawn parallel to the direction of the D_1 southwestward deformation; B: Cross-section drawn parallel to the direction of the D_2 northwestward deformation; C: Seismic profile parallel to the D_2 extensional direction (re-interpretation from Wang et al., 1998b).

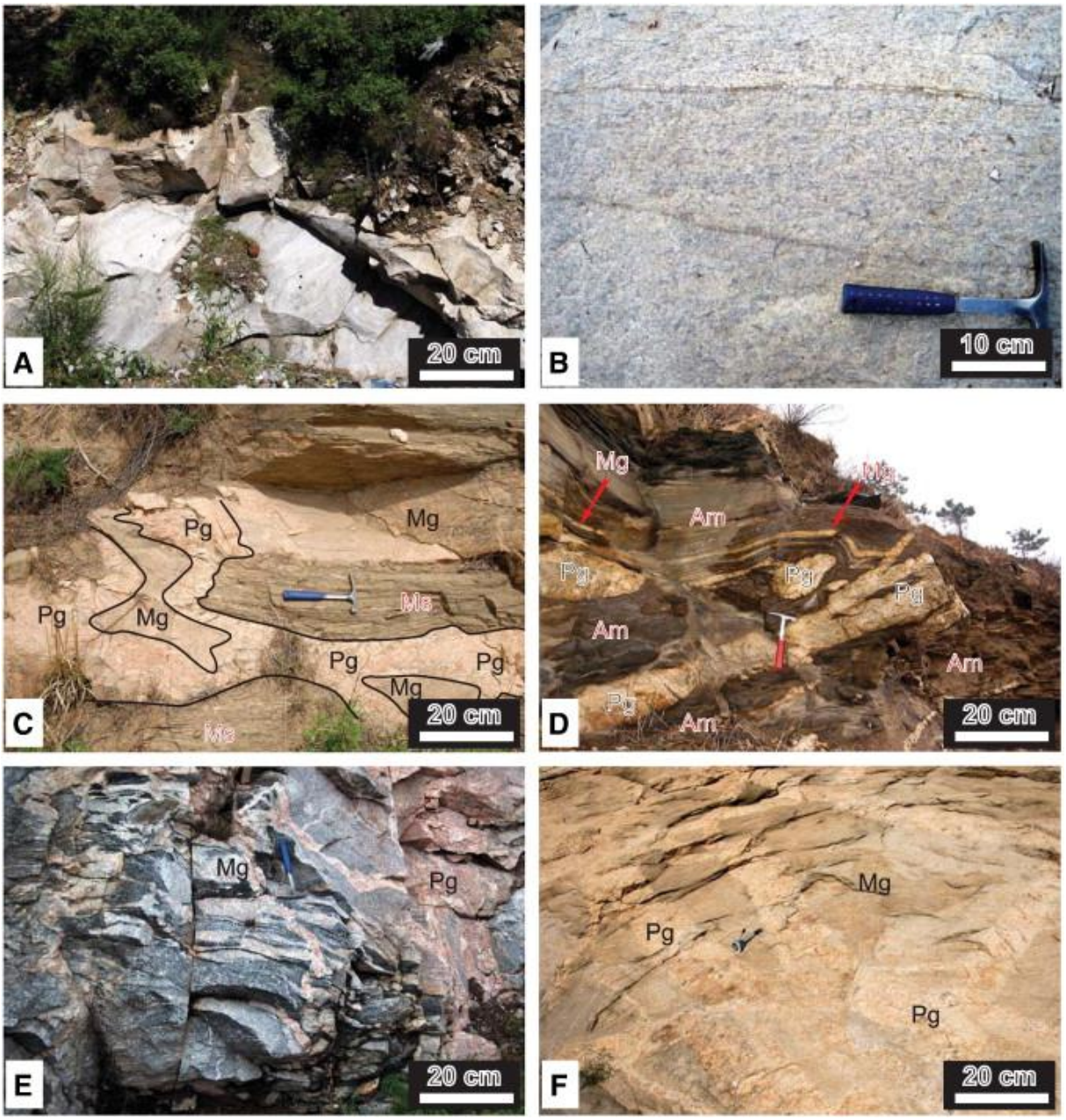

Fig. 4. Photographs showing the various lithologies of the Yiwulüshan massif. A. Magmatic foliation in the undeformed monzogranite (41°28.201′, 121°37.099′); B. Post-solidus lineation in the foliated monzogranite (41°37.560′, 121°28.561′); C. Undeformed pegmatite (Pg) intrusive into the foliated micaschist (Ms) and Monzogranite (Mg) (41°22.241′, 121°30.588′); D. Unfolded pegmatite vein and boudinaged pegmatite (Pg), the later cut the well foliated amphibolite (Am) and foliated interlayered monzogranite (Mg) intrusion (41°32.590′, 121°33.678′); E. Pegmatite vein cutting the undeformed granodiorite and monzogranite vein (41°33.629′, 121°37.085′); F. Pegmatite vein intrusive into the unfoliated monzogranite massif (41°32.009′, 121°40.106′).

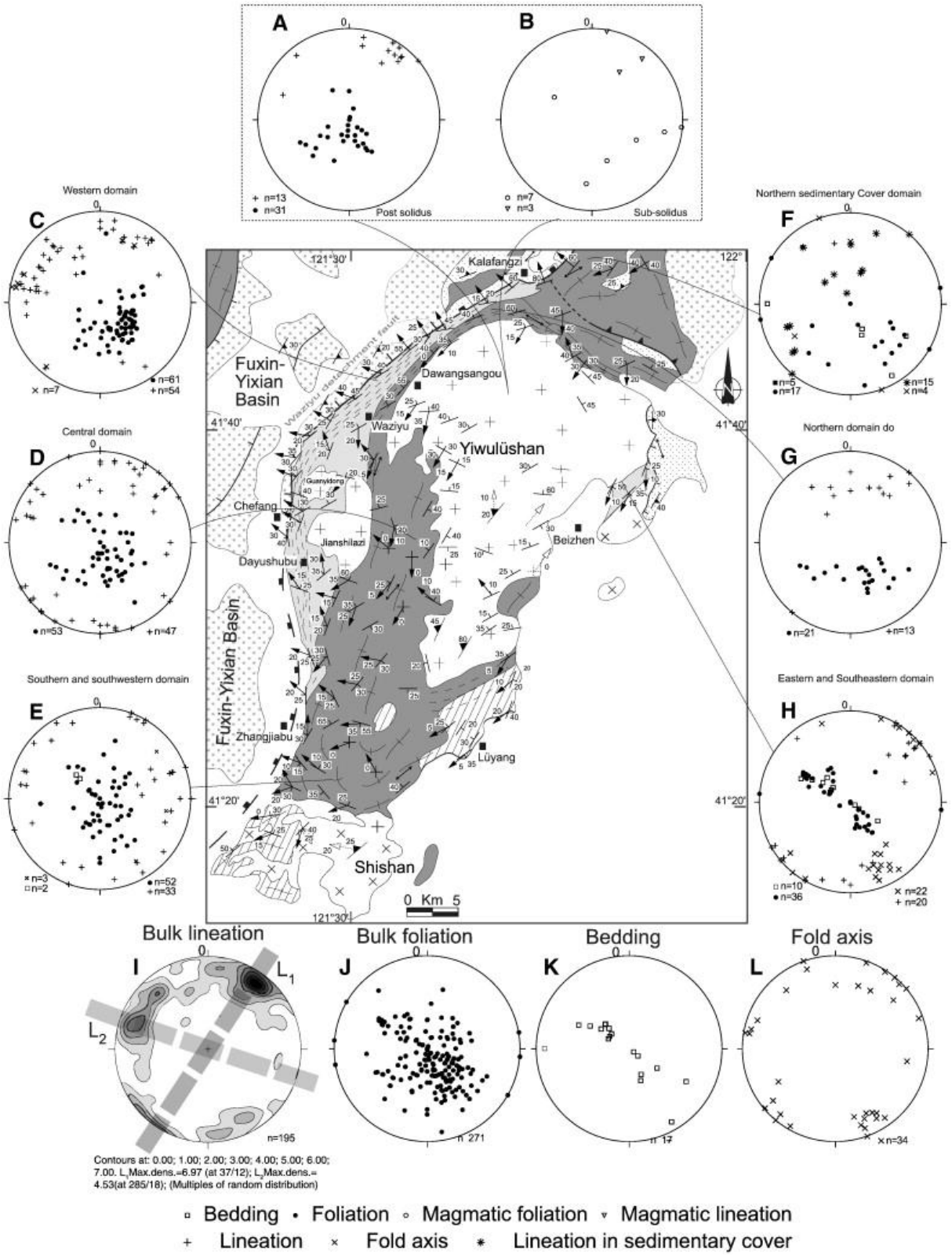

Fig. 5. Structural planar and linear elements of the Yiwulüshan Massif: bedding, foliation, mineral and stretching lineation and fold axis. All diagrams are equiareal Schmidt net, lower hemisphere (figure captions are the same in Fig. 2).

Around these granitoids, the Precambrian units comprise the Late Archean and Paleoproterozoic Jianping and Waziyu Groups, (Fig. 2). The Jianping Group is composed of monzogranitic gneiss, gneissic tonalite, biotitic plagio-amphibolite, biotitic plagio-gneiss, amphibolite, quartzite, and lenticular marble (LBGMR, 1989). The foliated, even mylonitic, monzogranitic gneiss and gneissic tonalite constitute the main part of this metamorphic unit (LNBGMR-Yixian, 1970). From a lithological point of view, it is difficult to separate the Archean monzogranitic gneiss and the foliated Jurassic monzogranite ([LNBGMR-Yixian, 1970] and [Wu et al., 2006]). The Waziyu Group, mainly exposed in the northwest, north and east of the massif, consists of micaschist, two-mica quartz-schist, sericite quartz-schist, quartzite, and metapelite (Fig. 2; LNBGMR-Yixian, 1970). In the NW part of the massif, near the Waziyu city, these rocks are strongly mylonitized with a well developped NE–SW striking foliation slightly plunging to the northwest, and a NW–SE striking mineral stretching lineation (Fig. 5C). In the north of the massif, the sedimentary bedding is preserved in Mesoproterozoic to Mesozoic slates, quartzites, limestones, dolomite, sandstone, and volcanic rocks (Fig. 2). These sedimentary strata are deformed by northwestward or westward verging folds (Fig. 2 and Fig. 3A, 5F). In spite of local structural disturbances by the Cretaceous intrusions or late faulting, the systematic measurement of the planar structures (bedding, slaty cleavage and foliation) shows that NE–SW planar structures progressively turn to the ENE–WSW to the west-northwest and southwest margins, and E–W in the northern and southern parts of the massif. This foliation pattern indicates a domal structure of the Yiwulüshan massif (Fig. 2 and Fig. 5J).

Granitic veins are well developed in the Yiwulüshan massif (Fig. 4C–F). Except the undeformed latest stage quartz vein, at least two stages of granitic veins can be separated on the basis of their mineralogical composition and deformation. Namely, 1) monzogranitic, tonalitic and granodiorite veins, and 2) pegmatite with K-feldspar megacrysts are recognized. The granitic veins of the first stage commonly intrude in the orthogneiss, amphibolite, and micaschist that form the country rocks of the Lüshan pluton. These granitic veins exhibit a foliation parallel to that of the country rocks (Fig. 4C,D). As the most abundant veins in the Yiwulüshan massif, the foliated monzogranitic veins often extend from several hundred of meters to several kilometers. In the mylonitic zone, these granitic veins are boudinaged (Fig. 6F,G). In the Lüshan pluton, undeformed granodiorite is cut by unfoliated granitic veins, indicating that the different granitic facies have different emplacement time (Fig. 4E). The K-feldspar megacrysts pegmatite veins of the secondary stage are not foliated at the scale of the entire massif (Figs. 4D,F). These features indicate that the pegmatite veins are not involved in the deformation responsible for the regional foliation.

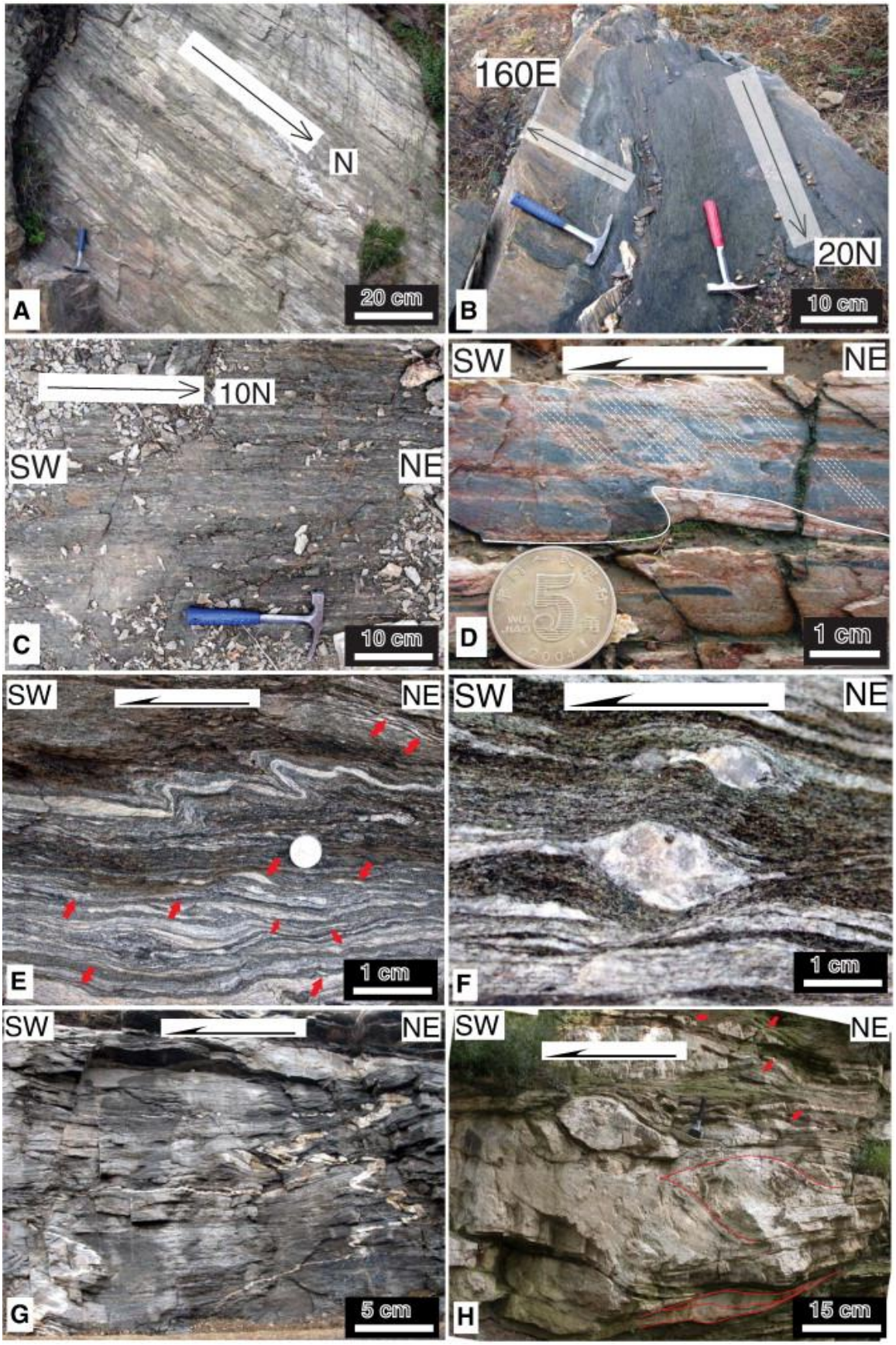

Fig. 6. Field-scale photographs related to Late Jurassic to Early Cretaceous top-to-the S or SW shearing (D_1 deformation): A: NE–SW trending stretching lineation in marble in a shear zone

developed in weakly metamorphosed Proterozoic sedimentary rocks, Kalafangzi (41°50.780′,121°43.040′); B: NE–SW trending mineral and stretching lineation formed by biotite and amphibole grains in a mylonitic amphibolite. Note that, in the granite vein (top-left), a NW–SE mineral and stretching lineation related to D_2 is developed, east of Dayushubu village (41°32.590′,121°33.678′); C: NE–SW trending mineral and stretching lineation formed by biotite, quartz and feldspar aggregates in the mylonitic gneissic tonalite, north of Lüyang city (41°23.732′,121°38.239′); D: SW verging folds with NE dipping axial planes subparallel to cleavage in the Proterozoic quartzite and quartzo-sandstone, northeast of Beizhen city (41°36.668′,121°52.460′); E: SW-vergent folds and sigmoidal quartz lenses in the mylonitic plagio-amphibolite and interlayered quartzo-felsic vein, north of Dawangshangou village (41°42.536′,121°34.992′); F: Sigma-type porphyroclast system of feldspar in mylonitic plagio-amphibolite and interlayered quartzo-felsic vein, north of Dawangshangou village (41°42.536′,121°34.992′); G: NW–SE folded, NE–SW boudinaged, and top-to-the SW sheared granitic vein in a mylonitic amphibolite, east of Dayushubu village (41°32.755′,121°33.613′); H: Meter scale D_1 shear zone developed in a monzogranitic sill intruding the host rock of Lüshan pluton, southeast of Dayushubu village (41°29.728′,121°31.288′).

In the western boundary of the Yiwulüshan massif, close to the Fuxin–Yixian basin, the well expressed foliation that strikes NE–SW, and plunges slightly (10°–45°, maximum around 18–22°, Fig. 5C) to the northwest is related to a several hectometers to kilometers thick shear zone called Waziyu or Sunjiawan–Shaohuyingzi detachment fault by Darby et al. (2004) and [Ma et al., 1999] and [Ma et al., 2000], respectively (Fig. 2 and Fig. 3C). This pervasive foliation contains a NW–SE striking mineral and stretching lineation, well marked by the preferred orientation of biotite, amphibole, K-feldspar, and quartz aggregates (Fig. 5C). More to the west, this fault prolongates under the Cretaceous Fuxin–Yixian basin with a low angle (Fig. 3C).

3.2. Polyphase deformation

Our field structural analysis and laboratory geochronological work allow us to recognize at least four successive events (referred to as D_1 to D_4) that can be distinguished on the basis of the geometry, kinematics and structural styles of the relevant macro-, meso-, micro-structures, and their chronological attribution. The identification of several distinct stages has been made in order to clarify the different structures, but obviously, the D_2 to D_4 events correspond to the same dynamics, namely extensional tectonics that prevailed during the formation of the Yiwulüshan MCC.

3.2.1. Early stage compressional event (D_1)

Previous works argued that the Yiwulüshan massif was a MCC formed during a NW–SE extension, with a top-to-the-NW low-angle normal fault ([Ma et al., 1999], [Zhu et al., 2003] and [Darby et al., 2004]). In fact, this deformation (referred to as D_2, in the following), observed mainly in the western part of the Yiwulüshan massif, is not the first one. The heterogeneously deformed granites and their host rocks that compose the main part of the massif, exhibit a pervasive foliation (S_1), and ductile shear zones attributed to an earlier deformation event-D_1 (Figs. 3A, 4B). In the central part of the Yiwulüshan massif, the S_1 foliation, developed during D_1, is subhorizontal to moderately dipping to the north, the axial

planes of isoclinal folds strike WNW–ESE (Fig. 2 and Fig. 3A, 5A,C,D,E,F,G,H,J). In mylonitic monzogranite, orthogneiss, amphibolite, micaschist, quartzite, and metapelite, D_1 is also characterized by a NE–SW trending mineral and stretching lineation (L_1) (Fig. 5A,C,D,E,F,G,H,J), represented by oriented aggregates of quartz, feldspar, muscovite, biotite, amphibole, epidote and chlorite (Fig. 6A–C). This indicates that D_1 is coeval with a lower amphibolite to greenschist facies metamorphism.

3.2.1.1. D_1 deformation in the sedimentary cover

In the sedimentary rocks exposed in the northern, northeastern, and eastern parts of the Yiwulüshan massif (Fig. 2), the strongly folded and mylonitized sedimentary cover also recorded this early deformation stage but under low metamorphic conditions. It is limited to the recrystallization of sericite or chlorite in the Mesoproterozoic to Neoproterozoic carbonates sandstones and quartzites (Fig. 6A). Bedding is often overprinted by a slaty cleavage and by a NE–SW trending stretching lineation marked by elongated and recrystallized chlorite, sericite or quartz grains (Fig. 6A,D). Northeast of Beizhen city, SW verging folds with NE dipping axial planes subparallel to cleavage in the Proterozoic quartzite and quartz–sandstone indicate the same kinematics (Fig. 6D). In thin section, cut parallel to L_1 and perpendicular to S_1, several shear criteria, such as sigma-type quartz and plagioclase porphyroclasts and sericite and chlorite pressure shadows, can be observed in the mylonitic, but weakly metamorphosed pelitic rock (Fig. 7A).

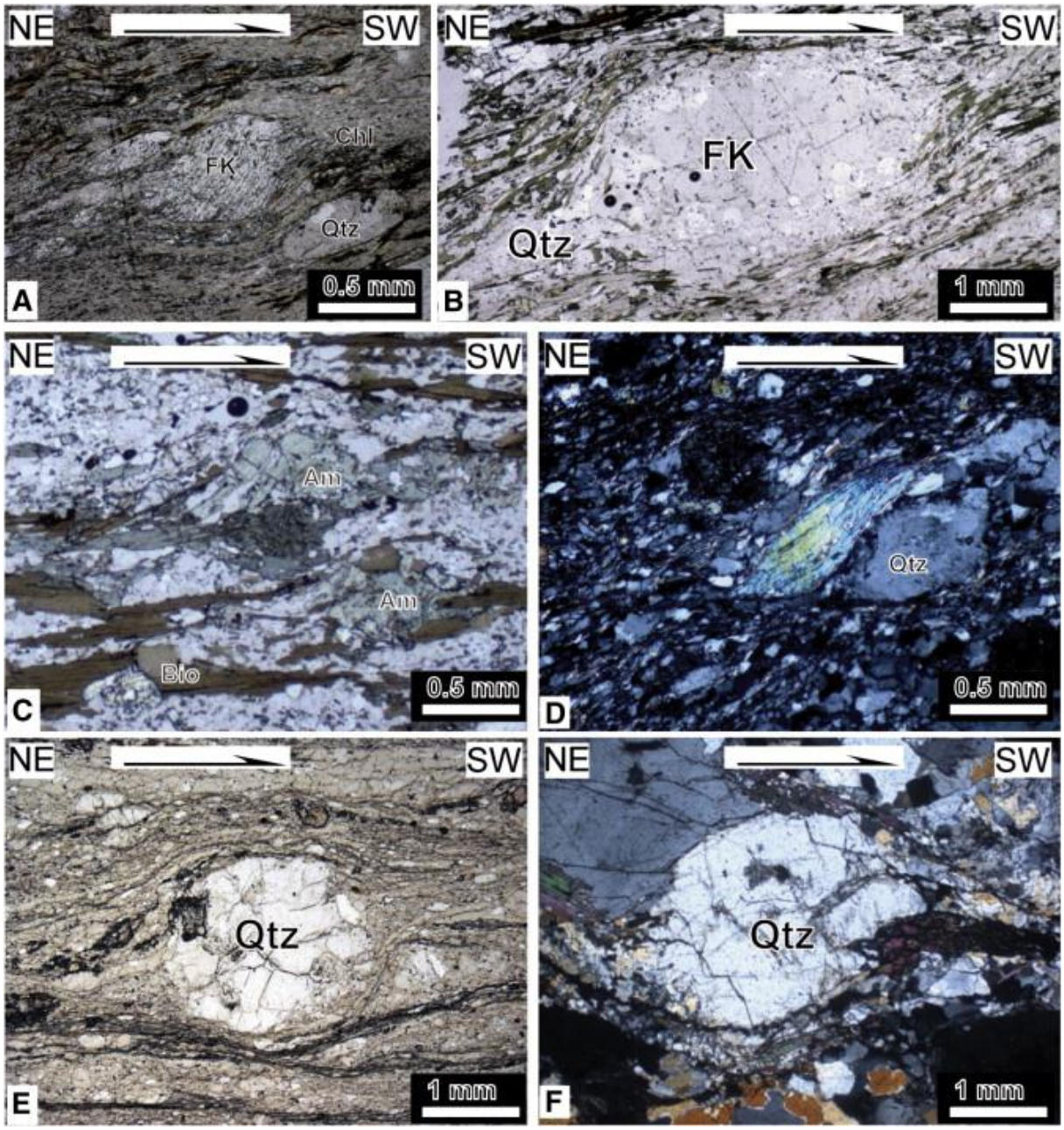

Fig. 7. Microphotographs showing shear criteria showing top-to-SW kinematics related to D_1 phase deformation from various lithologies: A: Sigma-type quartz and plagioclase porphyroclasts and related pressure shadows in a mylonitic weakly metamorphosed pelitic rock, north of Kalafangzi (41°51.405′,121°42.502′); B: Asymmetric pressure shadow around K-feldspar clast in a mylonitic plagio-amphibolite and interlayered quartzo-felsic vein, north of Dawangshangou (41°42.536′,121°34.992′); C: Sigmoidal amphibole porphyroclast and oriented biotite in a mylonitic plagio-amphibolite, South of Waziyu city (41°38.185′,121°29.100′); D: Mica (muscovite) fish in a mylonitic orthogneiss, northeast of Zhangjiabu (41°29.728′,121°31.288′); E: Sigma-type quartz porphyroclast in a mylonitic orthogneiss, northeast of Zhangjiabu (41°29.728′,121°31.288′); F: sigma-type porphyroclast system of quartz with asymmetric pressure shadow in a mylonitic monzogranite, south of Dawangshangou village (41°41.214′, 121°37.642′).

3.2.1.2. D_1 deformation in the basement rocks (micaschist, amphibolite and orthogneiss)

More to the south, micaschist, amphibolite, gneissic tonalite and monzogranitic gneiss occupy almost the half part of the Yiwulüshan massif (Fig. 2 and Fig. 3A,B). Though the foliation trend turns around the dome showing diverse dip directions, the mineral and stretching lineation L_1 is consistently oriented along a NE–SW strike with an average trend around N37°E (Fig. 2 and Fig. 5I,J, 6B,C). Whatever, the lithology: a top-to-the SW sense of shear is indicated by sigmoidal felsic veins, sigma-type K-feldspar, amphibole porphyroclasts, and SW-vergent folds at the outcrop scale (Fig. 6E,F,G,H). In thin section, mica (muscovite) fish and quartz, biotite, and amphibole in the pressure shadows around feldspar, amphibole and quartz clasts indicate the same kinematics at the scale of micro-structure (Fig. 7B–E). Under the microscope, quartz grains of mylonitic monzogranitic gneiss are intensely deformed by crystal–plastic mechanisms. For example, elongated quartz aggregates exhibit dynamic recrystallization microstructures such as core and mantle structure or serrated newly formed grains (Fig. 7D,F). Conversely, high strength minerals such as hornblende and K-feldspar are cataclastic and do not exhibit plastic deformation (Figs. 6F, 7C).

The Lattice Preferred Orientation (LPO) of quartz provides useful information of the deformation conditions. From North to South, sample CR 102 and Y 44 come from a quartz layer in mylonitic plagio-amphibolite. CR 100 is micaschists samples. Y 25 comes from a mylonitic plagio-amphibolite as xenolith in the mylonitic orthogneiss. Y 22 and Y 24 are a tonalitic orthogneiss (Fig. 8). The corresponding sub-fabrics (Fig. 8) exhibit some general characteristics. Namely, two diagrams have an orthorhombic symmetry with four suborthogonal point maxima, and three samples are dominated by a single point maximum. The location of points along the diagram edge, between the stretching lineation (X axis) and the foliation pole (Z axis) indicates that basal < a > gliding system is dominant. In agreement with natural and experimental data (e.g. [Etchecopar, 1977], [Law, 1990] and [Passchier and Trouw, 1996] and references therein), such quartz fabrics develop under low to middle temperature conditions (i.e. 300–400 °C). Therefore, these quartz c-axis fabrics likely developed subsequently to the peak metamorphism experienced by the gneisses of the Yiwulüshan massif. This conclusion agrees with the crystallization–deformation timing since, as shown above, shear criteria develop after the development of the metamorphic assemblages. The bulk kinematic picture provided by the quartz c-axis fabrics corresponds to non-coaxial flow in the entire massif (Fig. 8).

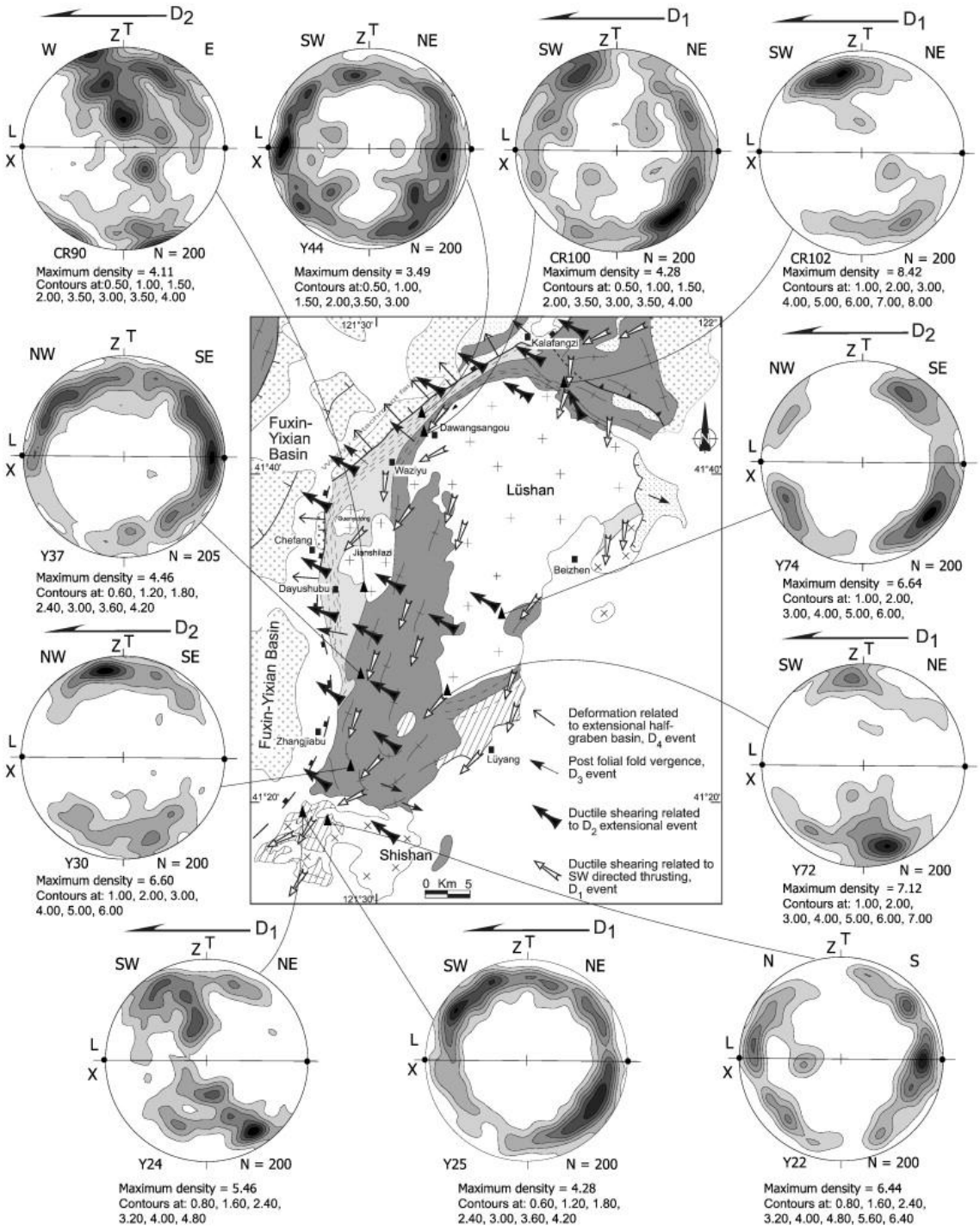

Fig. 8. Kinematic map for the different tectonic events in the Yiwulüshan massif and examples of quartz LPO obtained by universal stage measurement (figure captions are the same in Fig. 2). Arrows point to the sense of shear of the upper layer over the lower layer. Samples are foliated or mylonitic monzogranite (CR90, Y 72 and Y 74), quartz layer in mylonitic plagio-amphibolite (CR 102 and Y 37), and mylonitic plagio-amphibolite as xenolith in the mylonitic orthogneiss (Y 25), mylonitic plagio-amphibolite (Y 44), micaschist (CR 100), and mylonitic orthogneiss (Y 22, Y 24, and Y 30). All diagrams are lower hemisphere Schmidt net drawn in the XZ section of the bulk strain ellipsoid (e.g., perpendicular to foliation and parallel to the mineral and stretching lineation). Contour intervals given as multiple of random distribution are shown for each sample.

3.2.1.3. D_1 deformation in the Mesozoic monzogranite

Mesozoic monzogranite occupies almost half of the surface of the massif (Fig. 2). In the southern and western parts of the massif, the regional foliation exhibits a NE–SW trending mineral and stretching lineation L_1 (Fig. 2 and Fig. 5A). In the deformed granite, the mylonitization increases from the central part to the edge of the pluton. Low plunge foliation, and a NE–SW trending mineral and stretching lineation (L_1) are indicated by preferred orientation of feldspar, quartz, biotite and muscovite (Fig. 2 and Fig. 4B). Top-to-the-southwest the sense of shear is indicated by a meter scale shear zone at outcrop scale and sigma-type porphyroclast systems of quartz or asymmetric pressure shadow in the thin-sections and the LPO of quartz (Figs. 6H, 7F, and Y 72 of Fig. 8).

For the entire Yiwulüshan massif, the D_1 structures are observed in every litho-tectonic unit. All the kinematic criteria related to this early stage of deformation (D_1) show a top-to-the-SW sense of shear. The D_1 deformation is the dominant event in the Yiwulüshan massif, even if a late deformation stage (D_2) changed the geometry of the western part of the massif.

3.2.2. Main extensional deformation event (D_2)

In the western part of the massif, along the Kalafangzi–Waziyu–Chefang–Dayushubu area, a decameter to kilometer thick, flat-lying to west or northwest gently dipping, high strain shear zone developed (Fig. 2 and Fig. 3B, 3C). The NE–SW trending foliation exhibits a conspicuous mineral and stretching L_2 lineation with a dominantly NW–SE trend, and plunges slightly (10°–45°, the maximum around 20°) to the northwest (Fig. 2 and Fig. 5C–F). Mylonites are well developed in the metapelite micaschist and orthogneiss, which form the main part of the western massif, the sedimentary cover and the Mesozoic granites (Fig. 2 and Fig. 3C, 5). The previous workers interpreted this high strain zone as a detachment fault, named Waziyu or Sunjiawan–Shaohuyingzi fault, respectively ([Ma et al., 1999], [Ma et al., 2000] and [Darby et al., 2004]). NW–SE striking linear structures are indicated by the mineral and stretching lineation and the axes of intrafolial folds (Fig. 9A,B). The mineral and stretching lineation, L_2, which is marked by preferred orientation of biotite, muscovite, amphibole, epidote, K-feldspars and quartz aggregates, is consistently oriented along a NW–SE trend with a maximum around 285°/18° (Fig. 2 and Fig. 5C,D,E,I, 6B, 9A).

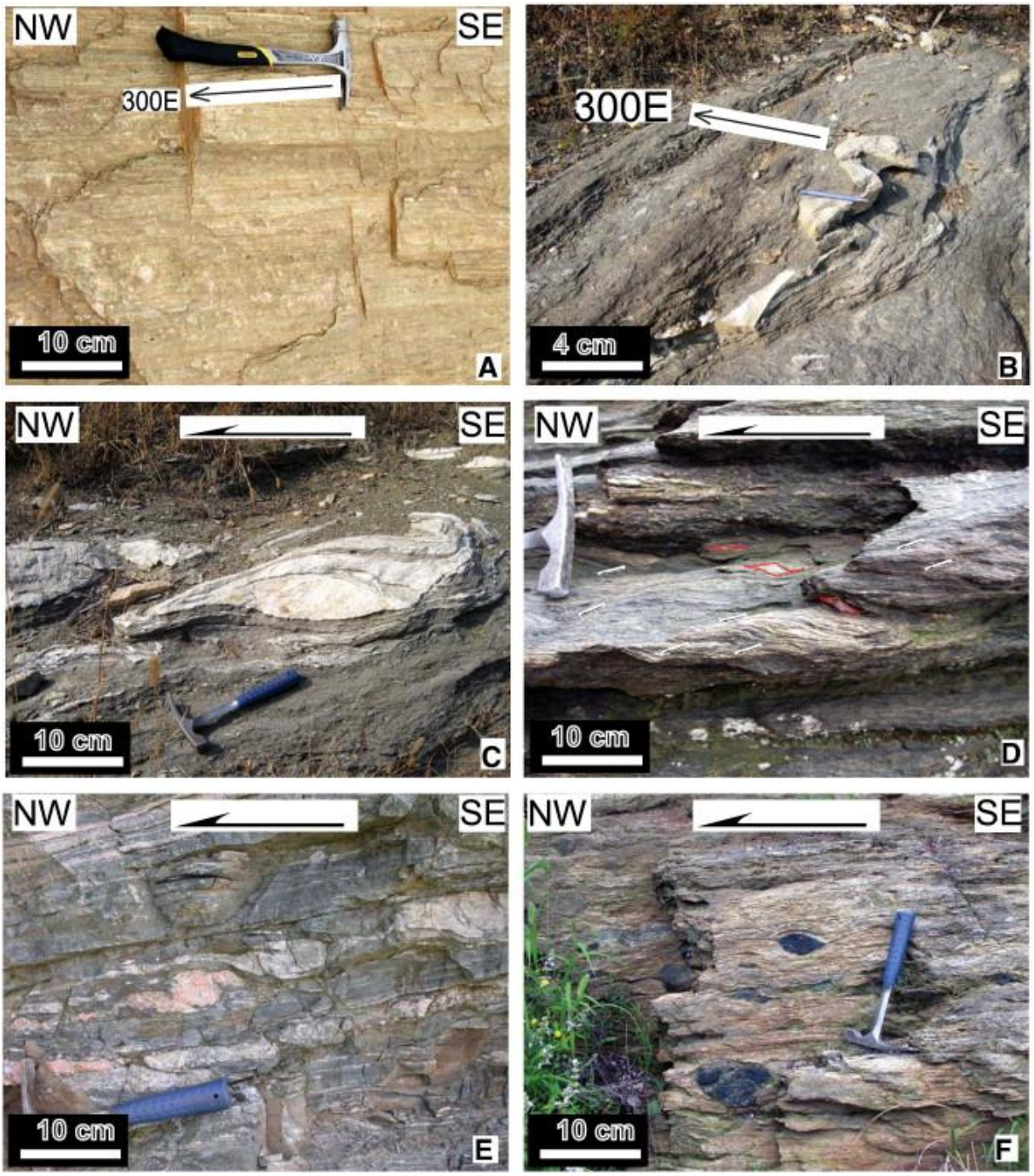

Fig. 9. Field-scale photographs related to the Early Cretaceous top-to-the NW shearing (D_2 deformation): A: Ultra-mylonitic foliation surface of monzogranitic orthogneiss holding a well pronounced NW–SE trending mineral and stretching lineation consisting of biotite, quartz and K-feldspar aggregates, east of Zhangjiabu city (41°27.447′,121°32.651′); B: Intrafolial folds of monzogranitic vein in the micaschist with axes parallel to the NW–SE trending D_2 regional stretching lineation, northeast of Chefang village (41°37.584′, 121°28.547′); C: Sigmoidal monzogranitic vein and NW verging intrafolial fold in mylonitic micaschist, northeast of Chefang village (41°37.584′, 121°28.547′); D: Sigmoidal interlayered quartzo-felsic vein and micaschist, and shear band indicating a top-to-the NW shearing along the Wuziyu detachment fault, northeast of Waziyu village (41°35.728′,121°27.394′); E: Asymmetric quartzose and felsic vein within the mylonitic amphibolite,

southeast of Dayushubu village (41°30.100′,121°29.855′); F: Sigmoidal mafic enclaves within the ultra-mylonitic monzogranite, northeast of Zhangjiabu city (41°27.959′,121°29.871′);.

Top-to-the-NW shear criteria are documented at the outcrop scale by sigmoidal granitic veins, shear band, and mafic enclaves within the ultra-mylonitic monzogranite (Fig. 8C,D,E,F). At the microstructural scale, the same kinematics is shown by sigma-type porphyroclast systems of plagioclase, quartz asymmetric pressure shadows and shear bands (Fig. 10A). Muscovite fish, shear bands, and quartz, chlorite, biotite, and amphibole asymmetric pressure shadows around muscovite, epidote, plagioclase, and quartz clasts in thin sections (Fig. 10B–G). Alike D_1 deformation, quartz grains involved in this D_2 deformation is deformed by crystal–plastic mechanisms. Conversely, the high strength minerals like epidote and K-feldspar are cataclastic, and do not exhibit plastic deformation (Fig. 10C,D). The LPO of quartz was used also to assess this D_2 stage deformation (Fig. 8). The LPO of quartz c-axes of deformed quartz aggregates and ribbons was analyzed using a universal stage for four localities from foliated monzogranite (Y 74), a quartz layer in mylonitic plagio-amphibolite (Y 37), orthogneiss (Y 30), and mylonitic monzogranite (CR 90) (Fig. 8). Three samples are dominated by a single point maximum indicating the activity of basal < a > gliding system. Such quartz fabrics develop under low to middle temperature conditions like the D_1 deformation (i.e. 300–400 °C).

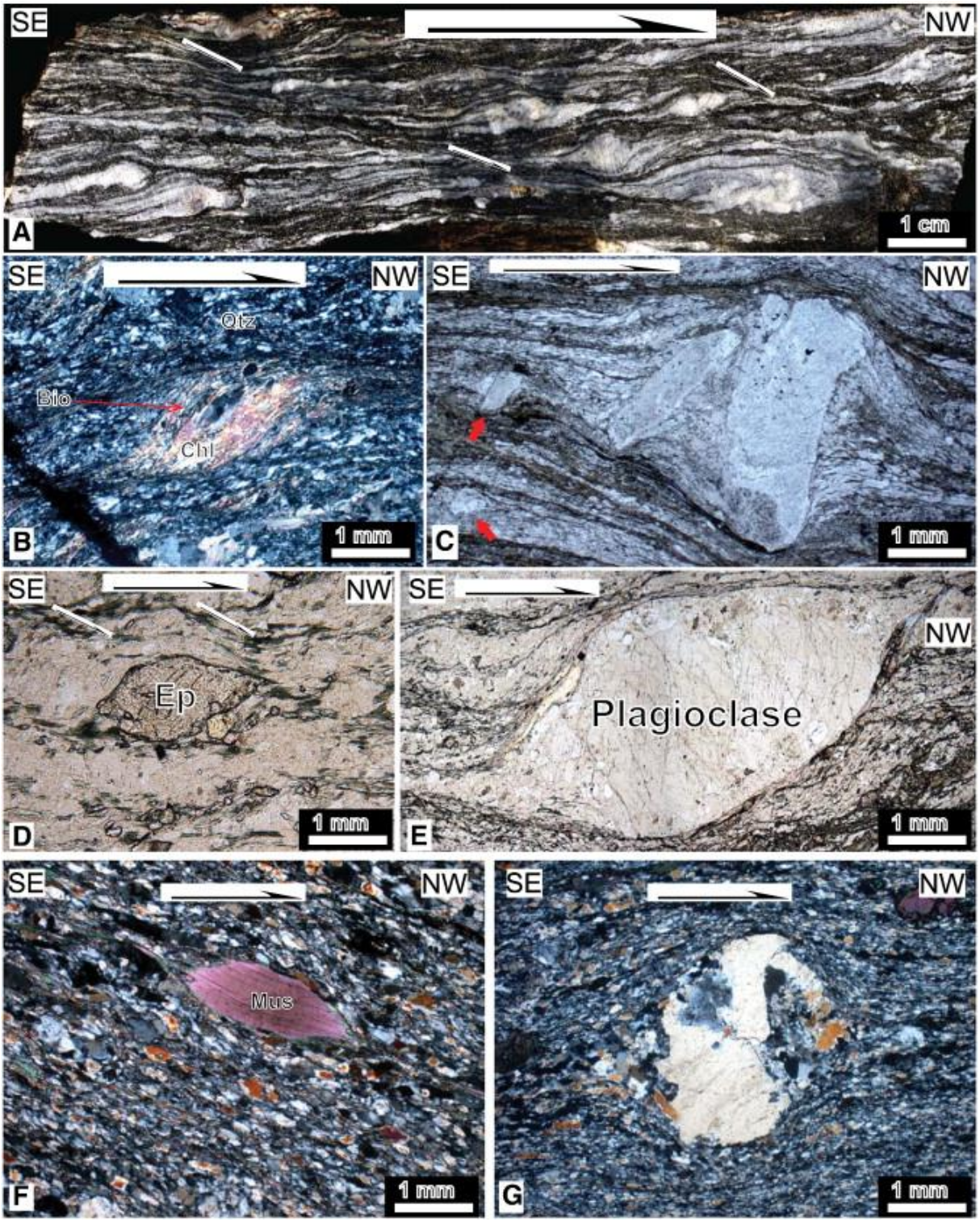

Fig. 10. Examples of top-to-the NW kinematics (D_2 deformation) at hand sample and microscope scales A: Sigma-type porphyroclast system of plagioclase with asymmetric pressure shadow and shear band in mylonitic micaschist involved into the Cretaceous detachment (Waziyu) fault, D_2 deformation, northeast of Waziyu (41°35.728',121°27.394'); B: Sigma-type quartz, muscovite, and chlorite porphyroclasts and related pressure shadows in a mylonitic weakly metamorphosed pelitic rock, north of Kalafangzi (41°50.288',121°43.555'); C: Asymmetric pressure shadow around plagioclase in a mylonitic weakly metamorphosed pelitic rock, north of Kalafangzi (41°50.288',121°43.555'); D: Sigma-type porphyroclast system of epidote with asymmetric pressure

shadow and shear band in mylonitic amphibolite, D_2 deformation, plagio-amphibolite, northeast of Zhangjiabu (41°30.100′,121°29.855′); E: Asymmetric pressure shadow around plagioclase in mylonitic amphibolite, D_2 deformation, northeast of Zhangjiabu (41°30.100′,121°29.855′). F: Mica (muscovite) fish in a mylonitic orthogneiss, southeast of Dayushubu (41°32.139′,121°30.529′); G: Sigma-type porphyroclast system of quartz with asymmetric pressure shadow in a mylonitic orthogneiss, southeast of Dayushubu (41°32.139′,121°30.529′).

It is worth to note that, in the sedimentary rocks exposed in the northern part of the Yiwulüshan massif (Fig. 2), the metamorphism is weak, only represented by the recrystallization of sericite or chlorite in the Mesoproterozoic sandstone, pelites, muddy limestones or dolomite. Along this L_2 lineation, a top-to-the-northwest sense of shear is indicated by sigma-type quartz, muscovite, and chlorite porphyroclasts and asymmetric pressure shadow around plagioclase (Fig. 10B,C).

To the western side of the Yiwulüshan massif, the top-to-the-northwest kinematics is in agreement with the normal fault displacement: the sedimentary cover is moving downwards to the west. We consider that the geometry and kinematics of D_2 event is related to the exhumation of the Yiwulüshan massif. It is worth to mention that the D_2 deformation is globally devoid in the eastern part of the massif (Fig. 2). However, several decacentimeter-scale shear zone with NW–SE trending mineral and stretching lineation are recognized (Fig. 2), and our AMS work in the NE of the Lüshan pluton reveals a NW–SE magnetic lineation L_{M2} due to a secondary magnetic fabric related to a solid-state deformation (Lin et al., this issue). These structures indicate that even the main detachment fault is not arched in the eastern part of massif, as a subbranch, several splays related to this D_2 deformation had marked at this part (Fig. 3B).

3.2.3. Gravity collapse folding-Late doming deformation (D_3)

Another late deformation (D_3) corresponds to the folding of the planar and linear structures formed during the D_1 and D_2 event. This D_3 event is characterized by different structures depending on the lithology. In the eastern part of the massif, in the sedimentary cover, Neoproterozoic quartzite and marble are deformed by NE–SW trending, and east or southeast verging drag folds (Fig. 11A). They are related to the southeastward displacement, normal motion of the eastern flank of the Yiwulüshan massif. In the gneissic amphibolite, southeast vergent recumbent folds with centimeter scale axial planar cleavage that deformed the D_1 foliation are also attributed to the D_3 event (Figs. 11B, 5H). Similar structures are observed in the northwestern part of the massif, WNW vergent drags folds develop within the Proterozoic pelitic schist and granitic vein (Fig. 11C). North of Waziyu city, the D_2 foliation and lineation deformed by NW vergent folds indicate a normal motion of the western flank of the massif (Fig. 11D). The D_3 folds can be seen as gravity-driven drag-folds due to the collapse of the tilted series once they have reached the critical dip that allows folding of the bedding and the pre-D_3 foliations. Therefore, at the scale of the whole massif, the post-folial folds in the metamorphic rocks, and some of the recumbent folds in the sedimentary cover are overturned to the southeast in the southeastern part of the massif, and to the northwest in the northwestern part, respectively.

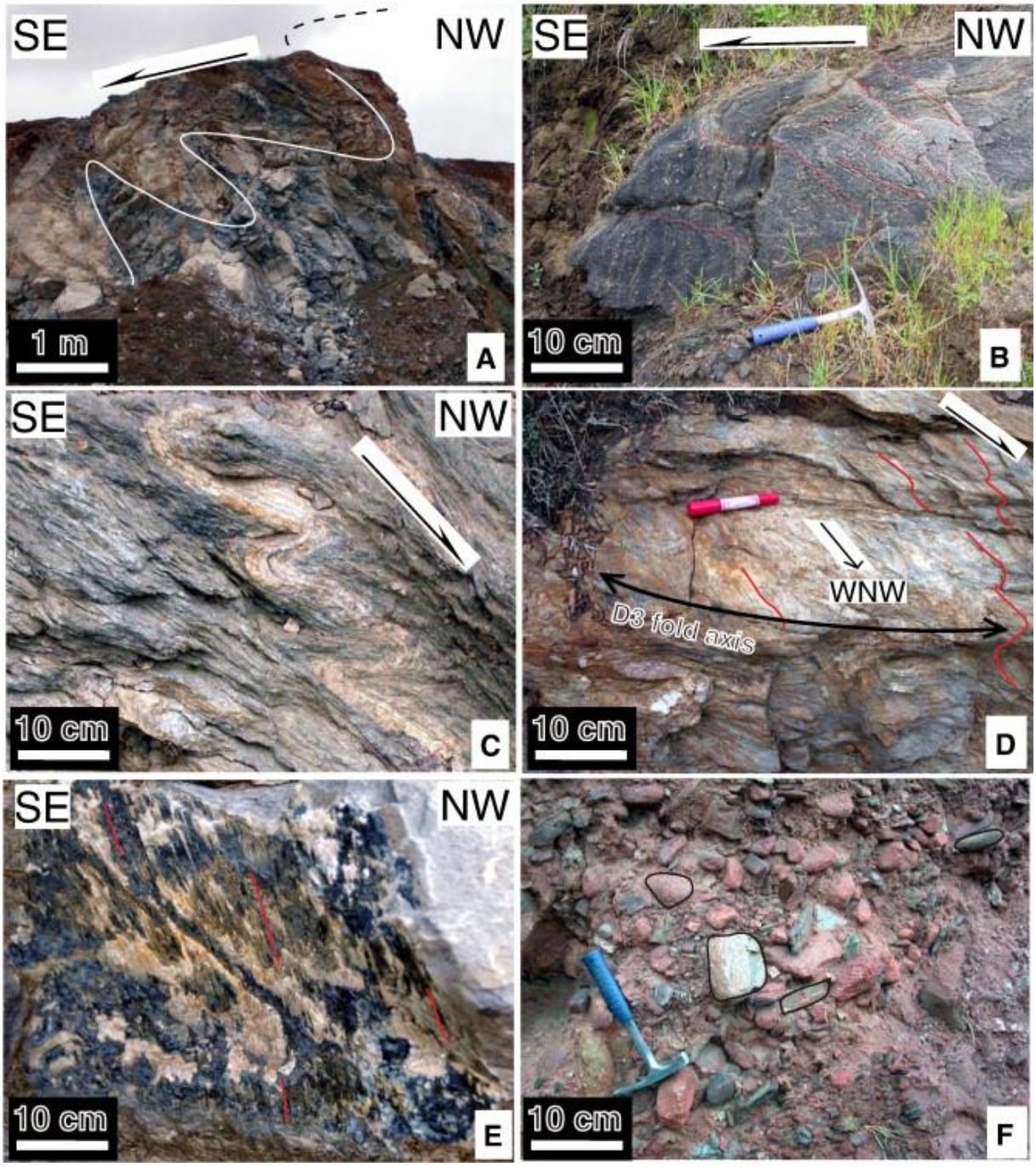

Fig. 11. Field-scale photographs related to gravity collapse folding (D_3 deformation) and brittle normal faulting (D_4 deformation): A: D_3 related meter-scale fold overturned to the southeast in Proterozoic quartzite and marble in the eastern edge of the massif, northeast of Beizhen city (41°39.536′,121°53.731′); B: D_3 related SE vergent recumbent fold with centimeter scale axial planar cleavage in gneissic amphibolite in the eastern edge of the massif, southeast of Lüyang city (41°20.510′,121°34.758′); C: NW vergent drag folds developing within Proterozoic pelitic schist and granitic vein related to the D_3 deformation, western edge of the massif, north of Kalafangzi (41°50.228′,121°43.555′); D: D_2 foliation and lineation deformed by NW vergent folds related to the D_3 deformation in the micaschist, western edge of the massif, north of Waziyu city (41°41.965′,121°31.752′); E: Slickenline and fault striae related to the D_4 deformation, western edge of the massif, north of Waziyu city (41°35.728′,121°27.394′); F: Pebbles of the mylonitic orthogneiss,

amphibolite, micaschist, pelitic schist, and undeformed granite situated at the upper most part of Early Cretaceous conglomerate (Sunjiawan formation-LBGMR, 1989), northwest of Wuziyu city (41°44.520′,121°33.828′).

At the scale of the Yiwulüshan massif, these northwest or southeast-vergent D_3 folds observed in the metamorphic core and in the sedimentary cover are interpreted as the later stage of the same tectonic event that is also responsible for the D_2 deformation. The generally flat-lying attitude of the axial planes is in agreement with a vertical shortening. Thus, the transition from D_2 to D_3 likely corresponds to the exhumation of the deep levels with a progressive tilting and partly arching of the detachment fault.

3.2.4. Brittle extensional faulting and related basin-forming Late doming deformation (D_4)

In the western margin of the Yiwulüshan massif, a brittle deformation zone separates the metamorphic rocks from the sedimentary rocks of the Early Cretaceous Fuxin–Yixian basin (Fig. 2 and Fig. 3B,C). This deformation is represented by high-angle brittle faults. In previous works, the Sunjianwan–Shaohuyingzi fault was undistinguishable used to describe both the brittle and ductile deformations ([LBGMR, Liaoning Bureau of Geology and Mineral Resources, 1989], [Ma et al., 1999], [Ma et al., 2000] and [Zhu et al., 2003]). Because the ductile fault was named Waziyu detachment fault (Darby et al., 2004), the Sunjianwan–Shaohuyingzi fault is preferred here to describe the brittle fault. Along this high-angle brittle fault, west to northwest-dipping planes bear striations trending about N290°E, i.e. down-dip. Tension gashes, Riedel fractures and offset markers indicate normal displacement (Fig. 11E). These normal faults represent the eastern boundary of the Fuxin–Yixian graben to half-graben. Inside the basin, a progressive increase of the proportion of coarse deposits (i.e. red sandstone and conglomerate) is observed when approaching the fault.

The sedimentological features and the tilt of the beds towards the fault suggest that normal faulting was coeval with the sedimentary infill of the half-graben basin (Fig. 3B). In summary, the D_4 brittle normal faulting deforms the D_2 foliation, which is folded during D_3. These D_2 to D_4 events represent the same extensional tectonics, however, pebbles of the mylonitic orthogneiss, amphibolite, micaschist, pelitic schist, and undeformed granite are observed in the uppermost part of Early Cretaceous conglomerate (Sunjiawan formation) (Fig. 11F; Peng et al., 2003).

4. Geochronological constraints

During the field work, several samples were collected from the Yiwulüshan massif in order to constrain the timing of the different tectonics events (Table 1). Nine mineral samples have been dated with $^{40}Ar/^{39}Ar$ method using step-heating experiments mineral samples, which were carried out at IGGCAS (Institute of Geology and Geophysics, Chinese Academy of Sciences). One sample (CR 105) of monzogranite has been dated by U/Pb method on zircon via the measurements of U, Th and Pb, which were conducted *in situ* using the Cameca IMS-1280 secondary ion mass spectrometry (SIMS) at IGGCAS.

Table 1. Summary of the samples dated by $^{40}Ar/^{39}Ar$ method.

Sample	Rock type	Coordinates	Analyzed mineral	Total age (Ma)	Plateau age (Ma)	Inverse isochron age (Ma)	($^{40}Ar/^{36}Ar$)i	MSWD
Y 22	Mylonitized tonalitic gneiss	N 41°17.872′;E121°27.881′	Amphibole	143.0 ± 0.9	140.9 ± 1.8	140.4 ± 2.3	319.7 ± 51.7	11.88
Y 24	Mylonitized orthogneiss	N 41°18.516′; E121°25.415′	Biotite	96.5 ± 1.9	97.0 ± 1.7	96.6 ± 2.6	298.0 ± 10.5	4.63
Y 25	Enclave of amphibolite in mylonitized orthogneiss	N 41°18.516′; E121°25.415′	Amphibole	138.1 ± 0.8	137.7 ± 1.4	137.3 ± 1.5	318.9 ± 37.6	13.36
Y 37	Mylonitized plagio-amphibolite	N 41°29.596′; E121°31.893′	Biotite	126.4 ± 1.1	128.5 ± 1.9	128.9 ± 2.3	288.1 ± 23.6	22.01
Y 44	Mylonitized amphibolite	N 41°42.536′; E121°34.922′	Biotite	111.4 ± 1.8	–	–	–	–
Y 44	Mylonitized amphibolite	N 41°42.536′; E121°34.922′	Muscovite	121.8 ± 0.7	121.1 ± 0.7	120.9 ± 0.7	305.6 ± 10.1	1.71
Y 71	Mylonitized micaschist	N 41°23.732′; E121°38.239′	Biotite	150.9 ± 1.5	–	–	–	–
Y 72	Gneissic monzogranite	N 41°26.187′; E121°35.940′	Biotite	133.8 ± 1.9	138.7 ± 1.8	140.2 ± 2.2	285.4 ± 10.2	5.95
CR 90	Mylonitized monzogranite	N 41°32.439′; E121°29.786′	Muscovite	118.4 ± 1.7	113.2 ± 1.3	112.9 ± 2.4	297.1 ± 10.7	3.35
CR 100	Mylonitized	N 41°42.532′; E121°34.988′	Muscovite	113.9 ± 4.2	107.1 ± 2.0	106.1 ± 3.0	299.5 ± 9.2	3.47

Sample	Rock type	Coordinates	Analyzed mineral	Total age (Ma)	Plateau age (Ma)	Inverse isochron age (Ma)	($^{40}Ar/^{36}Ar$)i	MSWD
	micaschist							
CR 100	Mylonitized micaschist	N 41°42.532′; E121°34.988′	Biotite	106.4 ± 2.2	98.4 ± 2.0	97.7 ± 4.0	296.5 ± 4.8	0.89

Sample descriptionY 22: Southwestern part of the massif. Mylonitized tonalitic gneiss with NE–SW mineral and stretching lineation (L_1) and top-to-the-SW sense of shear (D_1 deformation).Y 24 and Y 25: Southwestern border of massif. Mylonitic orthogneiss (Y 24) with sheared amphibolite boudin (Y 25). All these two samples with handle scale, NE–SE mineral and stretching lineation could be observed (L_1) and top-to-the-SW sense of shear (D_1 deformation).Y 37: Western part of massif. Mylonitic plagio-amphibolite which intrusive by the undeformed monzogranite. On the foliation of plagio-amphibolite, NW–SE (L_2) mineral and stretching lineation could be observed with top-to-the-NW kinematic (D_2 deformation).Y 44: Northwestern part of the massif. Mylonitic plagio-amphibolite and interlayered quartzo-felsic vein with NE–SW mineral and stretching lineation (L_1) and top-to-the-SW sense of shear (D_1 deformation, Figs. 6E,F, and 7B).Y 71: Southeastern part of the massif. Mylonitized gneissic tonalite with NE–SW mineral and stretching lineation (L_1) and top-to-the-SW sense of shear (D_1 deformation, Fig. 6C).Y 72: Southeastern part of the massif .Gneissic monzogranite with NE–SW mineral and stretching lineation (L_1) and LPO indicated top-to-the-SW sense of shear (Fig. 8; D_1 deformation).CR 90: Western part of massif. Mylonitized monzogranite with NE–SW mineral and stretching lineation (L_1) and top-to-the-SW sense of shear (D_1 deformation).CR 100: Northwestern part of the massif. Mylonitic micaschist and quartzo-schist with NE–SW mineral and stretching lineation (L_1) and top-to-the-SW sense of shear (D_1 deformation).

The detailed presentation of these data will be provided in another subsequent work, only the main results are given here (Fig. 12). Zircon yields a Late Jurassic age (160.4 ± 1.8 Ma), which is interpreted as that of the pluton emplacement. This result is in agreement with the previous results of Late Jurassic ([Darby et al., 2004], [Wu et al., 2006], [Du et al., 2007] and [Yin, 2007]). $^{40}Ar/^{39}Ar$ dating of amphibole, biotite, muscovite and K-feldspar give two groups of ages (Fig. 13). The earlier one, between 151 and 137 Ma, has a peak of statistic around 141 Ma defined from the amphibole, biotite and K-feldspar of the mylonitic tonalitic gneiss and amphibolite at the southern and eastern parts of the massif (Fig. 13). K-feldspar from mylonitic tonalitic gneiss yields a plateau age around 141 ± 1.0 Ma (Fig. 12). The late stage, between 129 and 97 Ma, is statistically defined around 126 Ma in the mylonitic orthogneiss, monzogranite, plagio-amphibolite and micaschist at the western and northwestern parts of the Yiwulüshan massif along the Waziyu detachment fault (Fig. 12 and Fig. 13). These two different group ages are considered to be the closest to the deformation ages of D_1 and D_2 events, respectively.

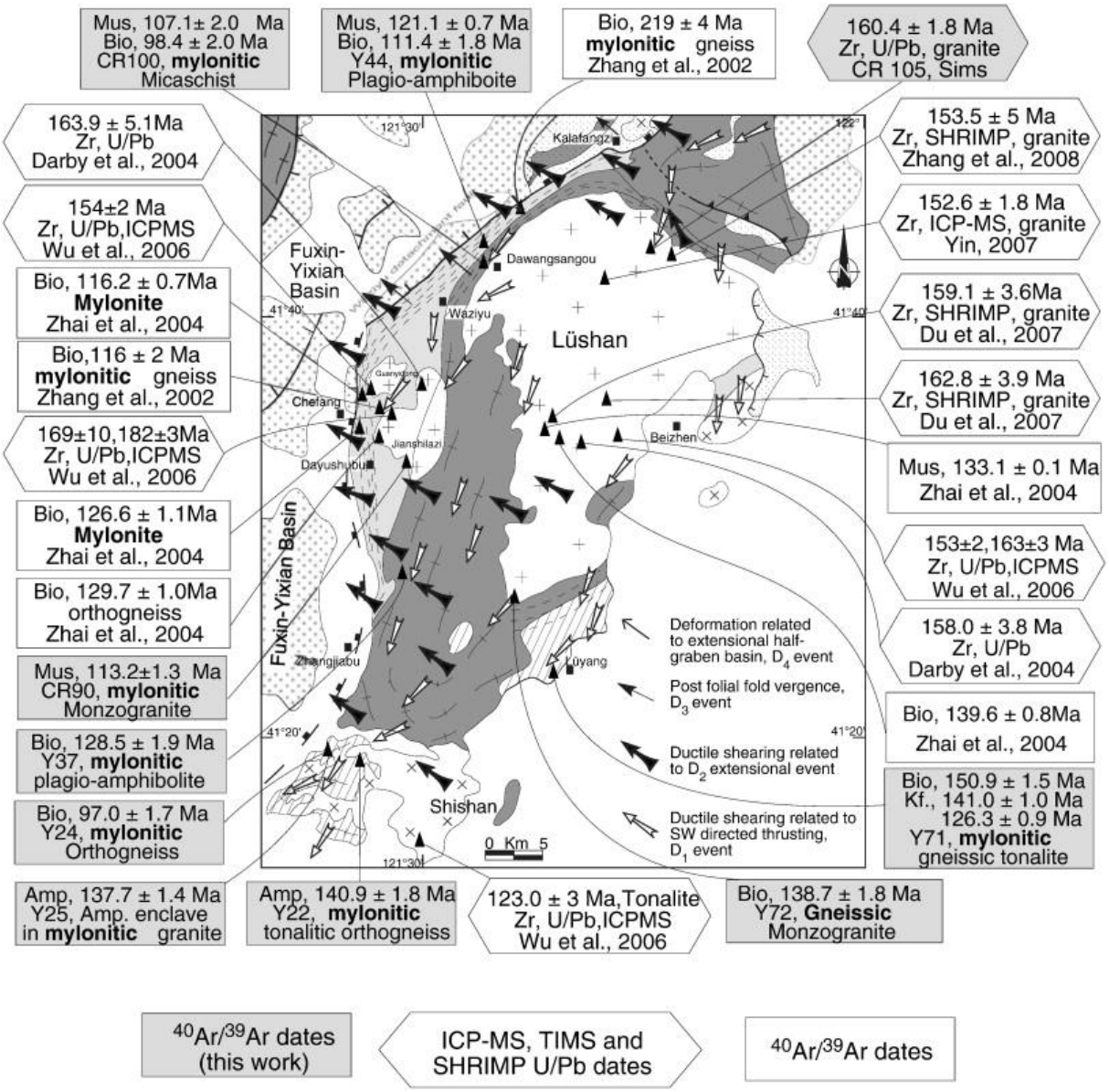

Fig. 12. Structural geological map with the kinematic component of the different tectonic events of the Yiwulüshan massif with the available radiometric ages (figure captions are the same in Fig. 2).

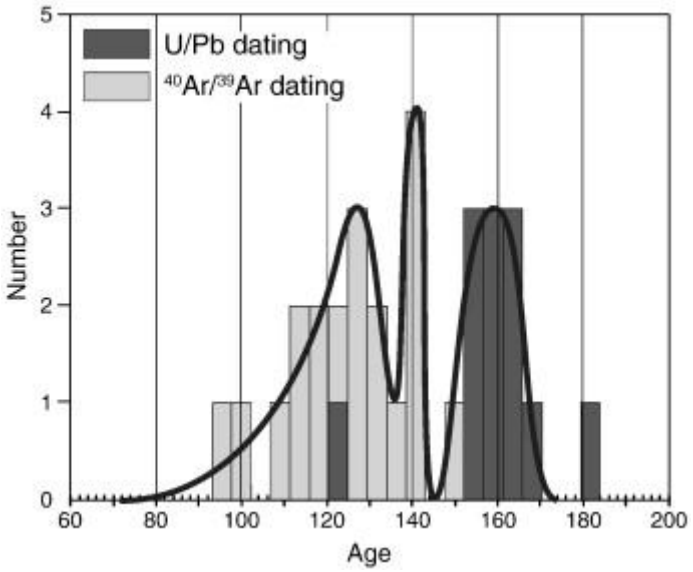

Fig. 13. Age probability diagram of the Mesozoic igneous rocks in the Yiwulüshan massif.

5. Discussion

5.1. Polyphase deformation and its geochronological constrain in Yiwulüshan—the MCC

The Yiwulüshan massif experienced several superimposed deformation events. The geometric and kinematic features related to each event described in the above sections are summarized in Fig. 14. Up to now, the D_1 deformation was poorly reported, especially in the Lüshan pluton. In fact, as mentioned before, the D_1 deformation is widespread in the Yiwulüshan massif. NE–SW mineral and stretching L_1 lineation and top-to-the-SW kinematics are not only recorded in the metamorphic rocks, but also in the sedimentary cover and in the Late Jurassic granitoids (Fig. 14). Our AMS work also documents a NE–SW magnetic lineation (L_{M1}, Lin et al., this issue). The D_1 event can be observed in every unit, except in the Cretaceous Fuxin–Yixian basin, and in the late intrusive tonalitic and adamellitic Shishan pluton. Thus, the D_1 deformation represents the main tectonic event of the Yiwulüshan massif, even if the primary architecture of the massif had been significantly modified by the D_2 event.

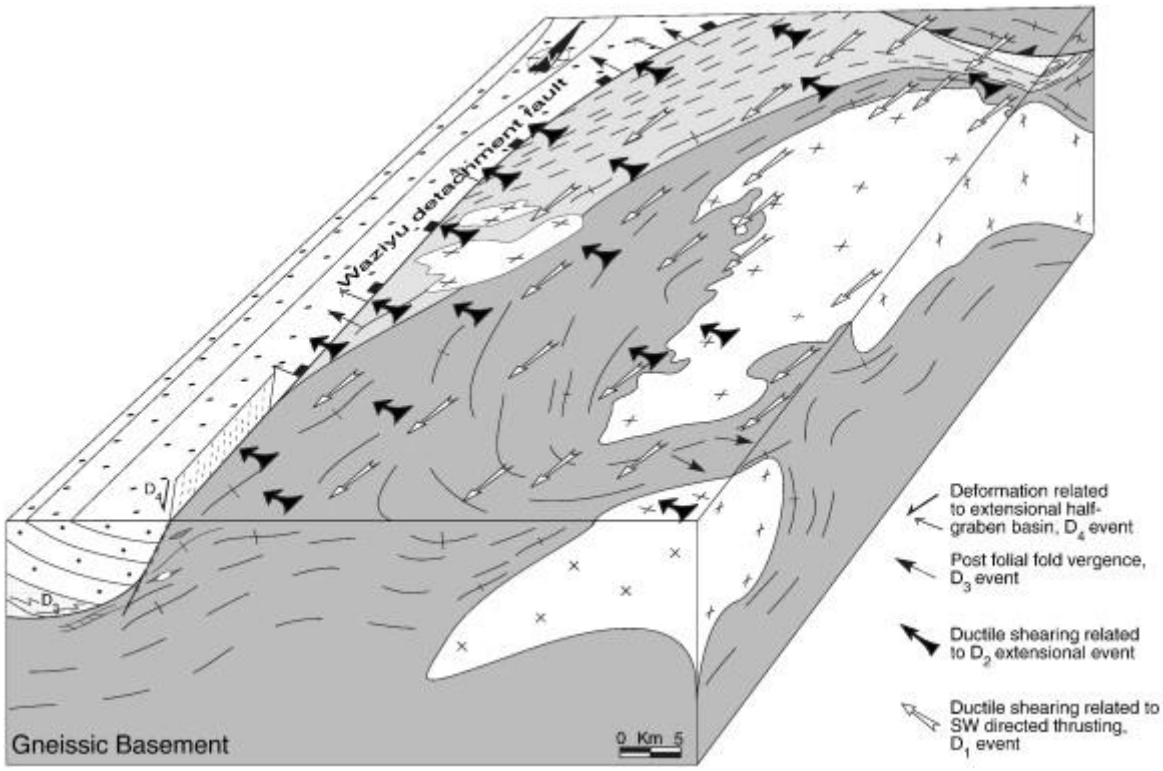

Fig. 14. Synthetic block diagram of the Yiwulüshan massif showing the bulk geometry and polyphase deformation (figure captions are the same in Fig. 2).

The age of this D_1 deformation is poorly established. Along the NE–SW L_1 mineral and stretching lineation, several radiometric ages have been determined in order to define the age of this main deformation (Fig. 12). Biotite, K-feldspar, and hornblende $^{40}Ar/^{39}Ar$ ages indicate a statistic peak around 141 Ma (Fig. 13). This result is in agreement with our work to establish the cooling path of the massif (Fig. 15). The combination the different mineral closure temperature form zircon U–Pb (800 °C) to K-feldspar multiple diffusion domain (MDD, 400–100 °C) indicates a "fast" cooling rate during this time (Fig. 15). The question will be raised whether this early Cretaceous D_1 deformation is due to compressional or extensional tectonics. Several lines of evidence lead us to consider that this tectonic event developed during a compressional tectonics. 1) Unlike the Waziyu fault of the D_2 event, an extensional detachment fault is absent in the south of the massif. 2) The geometry of the Lüshan pluton shows that the northern part is wider than the southern one. This suggests that the granite pluton is rooted to the north. The Bouguer gravity anomaly and gravity modeling support this structure (Fig. 2 and Fig. 3A; Lin et al., this issue). 3) The degree of anisotropy (P_j), which indicates that the mineral preferred orientation is higher in the southern than in the northern part of the massif (Lin et al., this issue), in agreement with a top-to-the-South shearing. 4) Similar top-to-the-south (southwest) compressional shearing of early Cretaceous age has been observed in the Miyun–Yunmengshan and Daqingshan areas, 400 km and 1000 km west from the research area, respectively ([Davis et al., 1996], [Davis et al., 2001], [Liu et al., 2002] and [Wang et al., 2011b]).

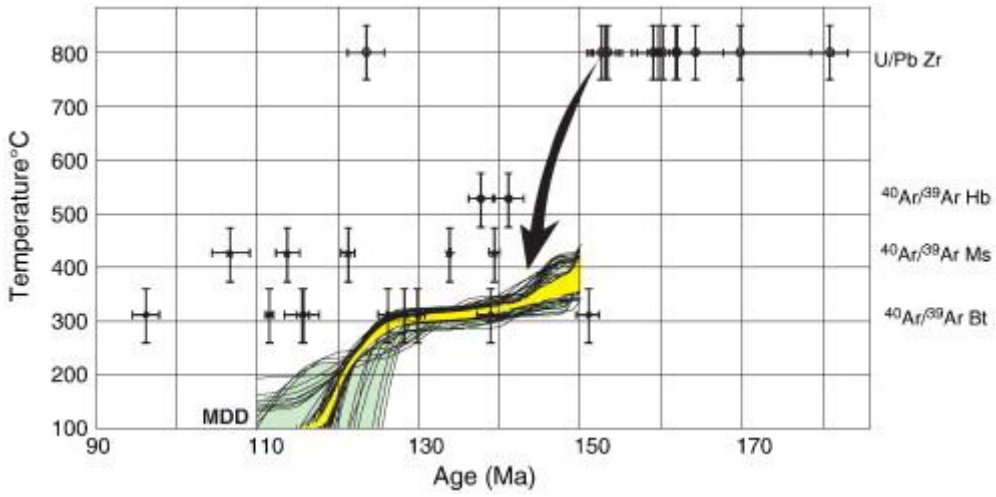

Fig. 15. Cooling paths of the Yiwulüshan massif, geochronological measurements come from the Fig. 12

Regionally, the D_2 deformation phase is observed along the western margin of the massif. The NW–SE trending mineral and stretching lineation and the top-to-the-NW kinematics are in agreement with a normal fault displacement ([Ma et al., 1999], [Ma et al., 2000], [Zhang et al., 2002], [Zhang et al., 2004], [Darby et al., 2004], [Liu et al., 2005] and [Lin and Wang, 2006]). This D_2 deformation is responsible for the construction of the final domal architecture of the Yiwulüshan massif, but it is not the most conspicuous deformation. Previous workers considered the D_2 event as concentrated along the Waziyu detachment fault ([Darby et al., 2004], [Liu et al., 2005] and [Lin and Wang, 2006]). After detail field survey in the central and eastern part of the massif, this NW–SE lineation and the top-to-the-NW kinematics is also observed in the mylonitic Jurassic monzogranite and host rock Precambrian gneiss (Fig. 2 and Fig. 3B, 5H and 8 (Y 74)). This structure is comparable with the Hohhot MCC, where the arched detachment fault is splayed into two parts ([Davis et al., 2002] and [Davis and Darby, 2010]). But in the Yiwulüshan massif, this warped detachment fault is limited at the centimeter to decacentimeter scale in the eastern part of the massif. Our AMS work confirms this observation (Lin et al., this issue).

Several radiometric ages of the D_2 deformation have been determined by previous works and our own $^{40}Ar/^{39}Ar$ measurement along the NW–SE mineral and stretching lineation (Fig. 12). Biotite and muscovite yield ages of $^{40}Ar/^{39}Ar$ from 129 to 97 Ma with peak of ages around 128–126 Ma (Fig. 13). We consider that the 128–126 Ma age approaches the true age of the Waziyu detachment fault, because this time was the beginning of the secondary fast cooling period from the view of K-feldspar multiple diffusion domain (Fig. 15). We argue that the 116–97 Ma ages correspond to the inhomogeneous cooling age of the minerals involved in the D_2 event.

At the scale of the whole Yiwulüshan massif, the D_3 deformation is represented by the west to northwest and east to southeast vergent folds with a flat-lying attitude of the axial planes. This geometric pattern allows us to define roughly the principal strain axes, characterized by NW–SE stretching (X axis) and vertical shortening (Z axis). As an important, but relatively limited deformation event, the D_4 event controls the opening of the Fuxin–Yixian basin as a supradetachment basin along the western trace of the Waziyu detachment. West-dipping normal faults that cut Neoproterozoic strata and micaschist in the hanging wall of the detachment fault north of Waziyu may be related to core complex development. Since the D_3

and D_4 structures have similar finite strain background, these two events are interpreted as the later stage of the same tectonic event responsible for the D_2 deformation. Thus, the rheological evolution from D_2 to D_4 likely corresponds to the same exhumation processes from the deep ductile levels to shallow brittle ones, along the detachment fault. This late stage structure is observed in many extensional structures, such as the South Liaodong Peninsula massif ([Lin and Wang, 2006], [Lin et al., 2008] and [Lin et al., 2011]). A similar evolution is also recognized in eastern China (e.g. [Faure et al., 1996], [Lin et al., 2000] and [Lin et al., 2008]).

Previous works (e.g. [Darby et al., 2004] and [Liu et al., 2005]) and our own structural and geochronological results allow us to summarize the main tectonic features of the Yiwulüshan massif. The geometry appears as an asymmetric metamorphic dome with a NE–SW trending long axis (Fig. 2, Fig. 3 and Fig. 5J). The dome bulk architecture and its kinematic pattern are controlled by the activity of D_1 and D_2 events. The upward arcuated shape of the mylonitic zones develops during the late stages of extension, in response to isostasy (e.g., [Spencer, 1984], [Lister and Davis, 1989] and [Wernicke, 1992]). The Waziyu detachment fault along west or northwest flank of Yiwulüshan massif is the master fault, whereas synformally folded faults to east or southeast are replaced by several limited splays of centimeter scale mylonitic zone in the Lüshan granite and micaschist and orthogneiss (Fig. 3B).

5.2. Regional significance of polyphase deformation–compression tectonics

The significance of the late Jurassic to early Cretaceous D_1 ductile event was not well worked in the Yiwulüshan massif (Darby et al., 2004). At the scale of the entire Yinshan–Yanshan orogenic belt, a late Jurassic to early Cretaceous top-to-the-south or southwest ductile thrusting is recognized north of Beijing, in Yunmengshan (Sihetang nappe) and Miyun area (pre-143 Ma to ≤ 127 Ma) ([Davis et al., 1996] and [Davis et al., 2001]).

In fact, a compressional deformation represented by fold and thrust structures has been mentioned in several places of Yinshan–Yanshan belt ([Wong, 1929], [Davis et al., 1996], [Davis et al., 1998], [Davis et al., 2001], [Chen, 1998], [Yang et al., 2001], [Darby, 2003], [Zhao et al., 2004], [Davis and Darby, 2010] and [Zhang et al., 2011]), the Southeast of Chengde city (Fig. 1), the Pingquan–Gubeikou thrust is a pre-early Middle Jurassic (> 180 Ma) South-directed structure ([Zhao, 1990] and [Davis et al., 2001]). The South vergent high-angle brittle Gubeikou reverse fault is dated between 148 and 132 Ma (Davis et al., 2001). In the Lingyuan–Qinglong area, 150 km west of Yiwulüshan massif (Fig. 1), late Triassic or pre-middle Jurassic polyphase deformations are recognized ([Davis et al., 2009] and [Hu et al., 2010]). But He et al. (1998) considered that the SE thrusting deformation occurred in late Jurassic.

As mentioned above, the Late Mesozoic Yinshan–Yanshan intra-continental orogenic belt exhibits unexplained structures such as multiple folds, thrust and reverse faults, extensional faults, strike-slips faults and a large volume of syn- to late kinematic plutons (Davis et al., 2001 and reference therein). The top-the-the-south (southwest) thrusting in the Yiwulüshan massif is comparable in time with the thrusts structures observed in the Yunmengshan and Miyun areas ([Davis et al., 1996], [Davis et al., 2001] and [Wang et al., 2011a]). Instead of the NE–SW trending of the Early Cretaceous basins, the sedimentation in the Jurassic basins, which develop along the Yinshan–Yanshan belt, with E–W or ENE–WSW axes, was terminated in the late stage of the Late Jurassic ([HBGMR, Hebei Bureau of Geology and Mineral Resources, 1989] and [He et al., 1998]). This marked a large compressional tectonic

period along the Yinshan–Yanshan belt during this time (Fig. 16). The geodynamic of this compressional deformation was related to the closure of the Mongol–Okhotsk Ocean, despite the fact that the distance between the suture and the belt is in excess of 1000 km ([Yin and Nie, 1996], [Davis et al., 2001] and [Metelkin et al., 2010]). But this hypothesis does not explain why there is no significant reactivation in the Solonker–Xilamulun belt, which is situated between the Mongol–Okhotsk and Yinshan–Yanshan belts, and was considered as the weakest zone because of the Paleozoic orogenic belt (Davis et al., 2004). The subduction of the Paleopacific or Pacific plate beneath Eastern Eurasian continent was also considered ([Xu and Wang, 1983], [Zhu et al., 2011a] and [Zhu et al., 2011b]), but this suggestion cannot explain the NE–SW direction of compressional deformation that is almost perpendicular to the direction of subduction. The influence of north–south Eurasian intraplate deformation and northwestward Pacific plate subduction and attendant arc magmatism (Davis et al., 2001) or formed independently of plate interactions in eastern Asia (e.g. Cui and Wu, 1997) was suggested to account for this puzzling compressional deformation. Nevertheless, the geodynamic explanations of the Late Jurassic–Early Cretaceous “Yanshanian” tectonics remain feeble.

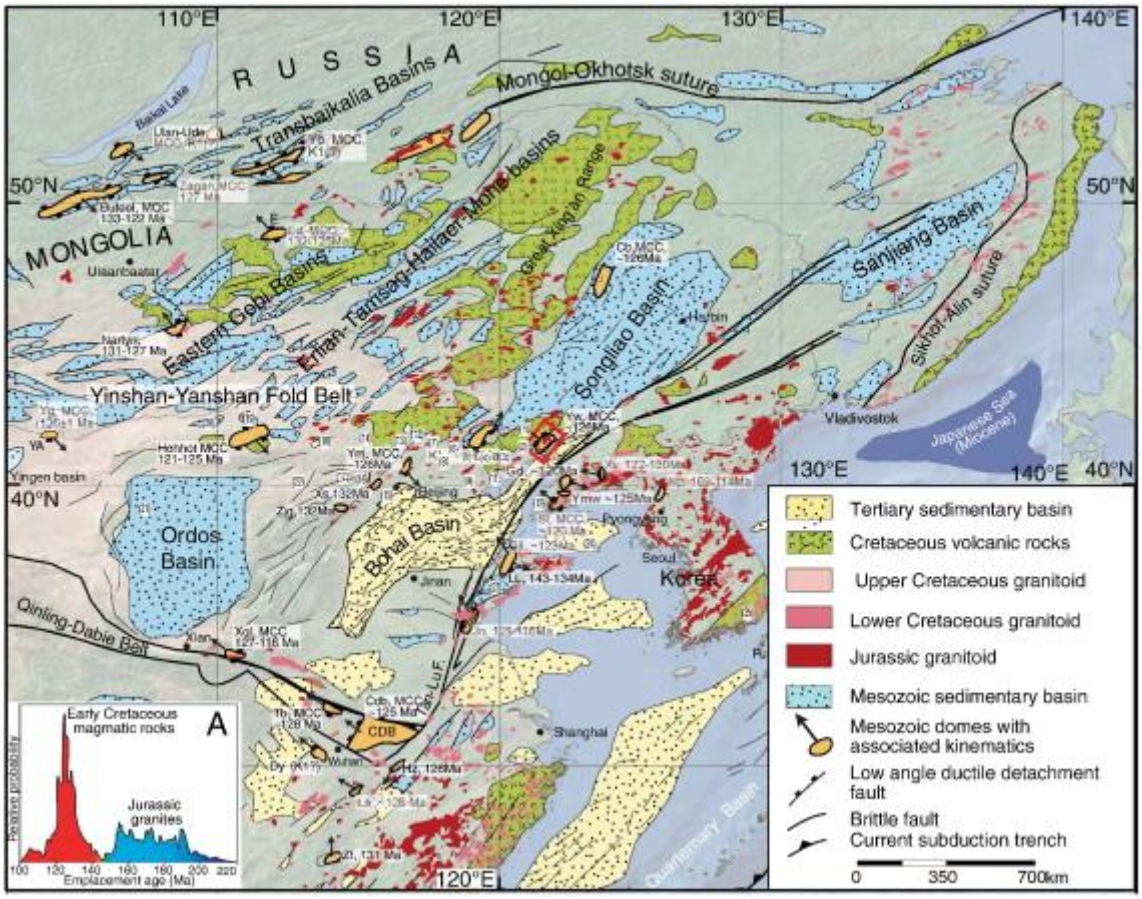

Fig. 16. Distribution of geological elements related to the Late Mesozoic extension at the eastern part of Eurasia continent (Modified from Charles, 2010): i) extension domes formed during Early Cretaceous: Yb (Yablonovy, Zorin, 1999); Buteel ([Mazukabzov et al., 2006] and [Donskaya et al., 2008]); Nartyn (magmatic dome, Daoudene et al., 2009), Zagan (Donskaya et al., 2008); Ed (Ereendavaa, [Daoudene et al., 2009] and [Daoudene et al., 2011]); Cb (Central basement uplift of Songliao basin, Zhang et al., 2000); Xy (Xiuyan magmatic dome, Lin et al., 2007); Yg (Yagan-Onch Hayrhan, [Zheng et al., 1991] and [Webb et al., 1999]); Hohhot ([Davis et al., 2002] and [Davis and Darby, 2010]); Kl (Kalaqin magmatic dome, Han et al., 2001); Ym (Yunmengshan, [Zheng et al., 1991], [Davis et al., 1996] and [Davis et al., 2002]); Yw (Yiwulüshan, [Darby et al., 2001], [Darby et al., 2004], [Zhang et al., 2002] and [Lin and Wang, 2006]); Xs (Xishan pluton, Wang et al., 2011c); Gd (Gudaoling syntectonic granite, [Guan et al., 2008] and [Lin et al., 2011]); Sl (South Liaodong Peninsula, [Yin and Nie, 1996], [Liu et al., 2005], [Lin and Wang, 2006] and [Lin et al., 2008]); Np (Nampho magmatic dome, Wu et al., 2007); Lg (Linglong–Guojialing complex dome, Charles et al., 2011); Jn (Jiaonan extensive dome, Hacker et al., 2009); Xql (Xiaoqinling MCC, Zhang et al., 1997); Cdb (Central Dabieshan MCC, Ji et al., 2011); Hz (Hongzhen magmatic dome Zhu et al., 2010); Ls (Lushan magmatic dome, Lin et al., 2000); Dy (Dayunshan syntectonic granite, Our field survey) and Zf (Syntectonic granite of Zhangfang in Wugongshan massif, Faure et al., 1996); ii) Late Jurassic to Early Cretaceous volcanics issued from Li (2000), Kirillova (2003), Meng (2003), Lin and Wang (2006), Wang et al. (2006), iii) Late Mesozoic continental red beds basin. (Modified from Traynor and Sladen (1995); [Allen et al., 1997] and [Lee, 1999]; [Ren et al., 2002], [Meng et al., 2003] and [Zhang et al., 2003]; Dill et al. (2004); Erdenetsogt et al. (2009)). A in the Fig. stand for the Age probability diagram of the

Mesozoic igneous rocks in eastern China, showing two important periods of magmatism in this area (from [Wang et al., 1998a], [Zorin, 1999], [Chough et al., 2000], [Li, 2000], [Wu et al., 2000], [Zhou and Li, 2000], [Davis et al., 2001], [Choi et al., 2005], [Wu et al., 2005a], [Wu et al., 2005b], [Wu et al., 2006], [Cheng et al., 2006], [Yang et al., 2006], [Zhou et al., 2006], [Wu et al., 2007] and [Wong et al., 2009] and references there in).

5.3. Cretaceous extension in the Eastern part of the Eurasian continent

The D_2 to D_4 events in the Yiwulüshan massif are related to the progressive extensional tectonics during the Cretaceous, which is recognized in a vast area in the eastern part of the Eurasian continent (Fig. 17). The presently documented MCCs, syntectonic plutons, detachment faults, and supradetachment basins are characterized by a NW–SE stretching, with either a top-to-the-northwest or a top-to-the-southeast sense of shear (Fig. 16). These extensional structures develop in the Transbaikalia–Mongolia–Great Xing'an range, Yinshan–Yanshan belt, Eastern China–Korea range (East of Tan-Lu fault), Qinling–Dabie belt and northern margin of the South China block (Fig. 17). The extensional metamorphic or magmatic domes indicated in the Fig. 17 are often associated with the formation of half-grabens developed in the detachment hanging walls (Fig. 3 and Fig. 17). The cooling period of MCC, geochronological dating of detachment faults and syntectonic plutons allow us to accurately define the time of this extensional tectonics (Fig. 17). In the Yiwulüshan massif, the detachment fault activity and pluton cooling age is around 126 Ma (Fig. 13). In the northern margin of SCB, the Hongzhen massif yields similar ages (Zhu et al., 2010). In eastern Liaoning province, the South Liaodong peninsula MCC has a younger, fast cooling period, between 121 and 114 Ma, and the syntectonic Gudaoling pluton has a fast cooling period between 118 and 114 Ma (Fig. 17; [Yang et al., 2008] and [Lin et al., 2011]). Because detailed geochronological work is lacking, the extensional period is imprecisely defined between the 135 and 120 Ma in the Transbaikalia–Mongolia–Great Xing'an range and North margin of the South China block (Fig. 16 and Fig. 17; [Donskaya et al., 2008], [Daoudene et al., 2009], [Daoudene et al., 2011], [Zhu et al., 2010] and [Ji et al., 2011]). On the contrary, in the Eastern Qingling–Dabieshan and Yinshan–Yanshan belt, it seems that the peak of extensional tectonics took place during 130–125 (Fig. 17). Eastern China and Korea (East of the Tan-Lu fault, EC of Fig. 17) this extensional event seems to have a larger time range, from 134 to 110 Ma, and a rapid cooling period at 122–114 Ma (Lin et al., 2011). This is slightly younger than in the other four areas (131–120 Ma, Fig. 17).

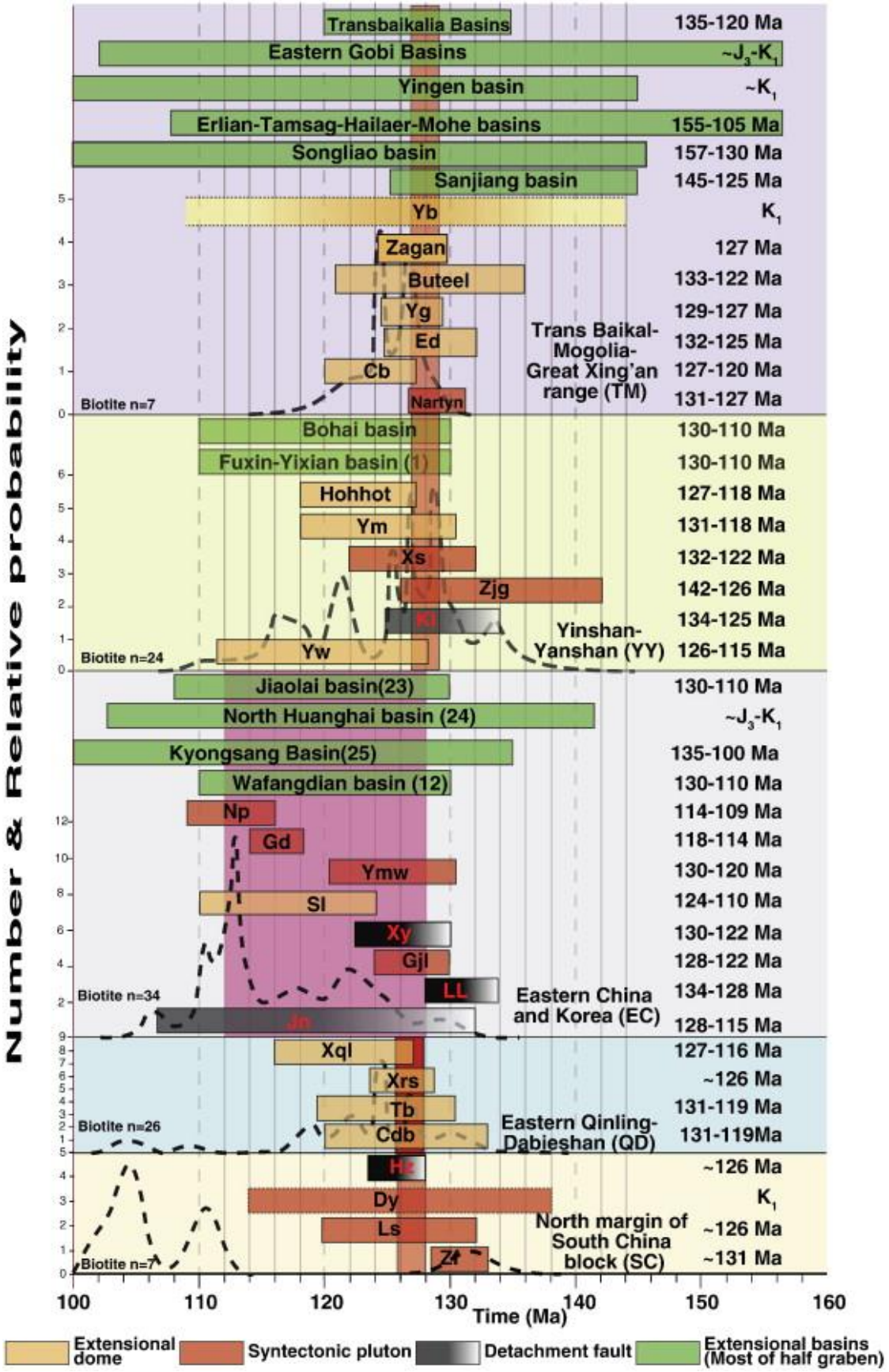

Fig. 17. Extensional structures (extensional dome, syntectonic plutons, detachment faults and basins), and their radiochronological ages in the eastern part of the Eurasian continent (the dash line

indicates the relative probability of the biotite ^{40}Ar–^{39}Ar dating on the ductile detachment faults). The times of formation of the metamorphic complexes and domes are indicated to reflect the active time of detachment fault. Information partly from Daoudene et al. (2011), additional information of extensional dome, syntectonic pluton, detachment fault and extensional basins from the same reference as in Fig. 16. Locations and the statistical data are indicated on Fig. 16 and its caption.

The origin of this continental-scale tectonic event is variously interpreted. Namely, 1) west-directed subduction of a Paleo-Pacific plate during the Mesozoic causes intra- or back-arc extension ([Watson et al., 1987], [Traynor and Sladen, 1995] and [Ren et al., 2002]); 2) roll-back of the westward subducting Paleo-Pacific oceanic plate, and post-orogenic collapse is following the Late Jurassic to Early Cretaceous contraction (Davis et al., 2001); 3) South-Southeast-directed subduction of the Mongol–Okhotsk oceanic plate during the Mesozoic is responsible for extension (Wang et al., 2002); 4) interaction between the Pacific back-arc spreading and a radial eastward tectonic escape resulting from the Lhasa block–West Burma–Qiangtang–Indochina collision ([Schmid et al., 1999] and [Ratschbacher et al., 2000]); 5) E–W extension coeval with N–S shortening in relation to collision along the northern and southern boundaries of the NCC ([Yin and Nie, 1996], [Gao et al., 2002] and [Zhang and Sun, 2002]); 6) post-orogenic thinning caused by gravitational collapse of a continental crust previously thickened during a collisional event ([Webb et al., 1999], [Zorin, 1999], [Graham et al., 2001], [Meng et al., 2003] and [Yang et al., 2005]); 7) thermal weakening due to Early Cretaceous magmatism (Darby et al., 2004) or 8) mantle plume ([Deng et al., 2004] and [Zhao et al., 2004]). If all the Early Cretaceous extensional structures have the same geodynamic origin, a scale problem arises since they are distributed all along the eastern part of Eurasia, over more than 1200 km across strike. Indeed, the distribution of MCC at the eastern part of Eurasia continent is much wider than the width of the Basin and Range Province in US where MCC is distributed parallel to the Cordilleran Orogenic Belt. In the eastern part of Eurasia continent, extensional structures do not exhibit a clear linear pattern, since they sporadically crop out in a vast area (Fig. 16). Neither of the hypotheses proposed above can completely account for the large extent of the continental crust involved in the early Cretaceous extension ([Watson et al., 1987], [Traynor and Sladen, 1995], [Ratschbacher et al., 2000], [Ren et al., 2002] and [Lin and Wang, 2006]). Back-arc extension or similar plate margin processes related to the subduction of a Paleo-Pacific plate is considered as the most active mechanism (Zhu et al., 2010 and reference therein). But these processes cannot explain the extensional features observed in the Transbaikalia–Mongolia–Great Xing'an range, the Yinshan–Yanshan belt, and the Qinling–Dabie belt, since these ranges are almost perpendicular the subduction direction. For the South China region, some of the previous workers attributed this Cretaceous event to mantle derived magma promoting thermal softening and gravitational extension (Faure et al., 1996), a rolling-hinge isostatic rebound during the eastward tectonic escape ([Schmid et al., 1999] and [Ratschbacher et al., 2000]) or asthenospheric upwelling through a gap opened by a detachment of slab and lithospheric root (Bryant et al., 2004). However, these models do not explain the similar extensional features situated in the NCC. The youngest event responsible for crustal thickening took place in the late Triassic, along the Tongbaishan, Dabieshan and Sulu ultrametamorphic belt, which is situated between the North China block and the South China block ([Zhang et al., 2001] and [Yang et al., 2005]) but the large time span, about 100 Ma, between the Late Triassic thickening and Cretaceous extension makes the explanation of the post-orogenic thinning unlikely.

Some authors related these extensional structures to a mantle plume ([Deng et al., 2004] and [Zhao et al., 2004]). However, such an interpretation is neither supported by the

regional architecture of the NCC nor geophysical data, since radial extensional structures are absent (Zhao and Xue, 2010). Furthermore, the high-resolution P wave tomography indicates that the subducting Pacific slab becomes stagnant in the mantle transition zone under east China (Huang and Zhao, 2006). This will make the model of the mantle plume rising from the lower mantle unlikely, as the stagnant slab will produce a screen that would not allow the plume to rise.

Intraplate or plate-margin processes appear unable to explain the Cretaceous continental-scale extension. As a matter of fact, mantle lithosphere removal (convective removal or delamination raised by the back-arc extension of the NW-direct subduction of Pacific plate) might account for the large continental area involved in extensional tectonics, occurring during a quite short time span in Late Mesozoic times (Lin and Wang, 2006). The partial loss of the lithospheric mantle would also be responsible for a significant uplift and the rise of a high plateau (Turner et al., 1996). Although such a plateau has been suggested for Mongolia and northeastern China in Cretaceous time ([Yin and Nie, 1996] and [Meng et al., 2003]), its topographic effect is not well recorded in the sedimentation since the amount of terrigeneous material deposited in the Cretaceous basins does not correspond to the important eroded volume of rock associated with such an uplift (Li et al., 1997). Moreover, the paleo-topographic evolution of the Cretaceous North China block remains poorly constrained. A more detailed discussion of the models of lithosphere removal is beyond the scope of this paper (c.f. Lin and Wang, 2006 for further discussion).

6. Conclusions

As a typical intraplate orogenic belt, the Yinshan–Yanshan belt remains poorly understood. The Yiwulüshan massif provides a good example of the Late Mesozoic succession of compressional and extensional tectonics experienced by the North China Block along the Yinshan–Yanshan belt. This massif combines polyphase synmetamorphic ductile shearing, synkinematic plutonism and half grabens formation. The early, south to southwest-directed thrusting, D_1 event is related to a compressional event recognized elsewhere in the Yinshan–Yanshan belt. The early Cretaceous tectonic, and plutonic events (D_2) recorded in the study area belong to the continental extension recognized in the central and eastern Eurasia. This early Cretaceous extensional deformation, subdivided into D_2, D_3 and D_4 events, is responsible for the final formation of the Yiwulüshan massif. The D_2 event, which corresponds to the northwestward normal ductile shearing around 126 Ma along the Waziyu detachment fault, accommodates the exhumation of the Precambrian basement and Jurassic plutons. The D_3 deformation is characterized by the development of gravity-driven recumbent folds affecting the micaschist, Neoproterozoic to Paleozoic sedimentary cover rocks, and partly arching of the detachment fault. D_4, which is restricted to the brittle normal faulting at the Eastern and Western sides of the massif reworks the mylonitic fabric developed during D_1. D_4 also controls the formation of Cretaceous continental Fuxin–Yixian graben.

The Yiwulüshan massif is the easternmost extensional dome recognized in the Yinshan–Yanshan belt. This extensional dome belongs to the widespread cretaceous extensional regime in the eastern part of Eurasian continent, in which a NW–SE trend of the maximum stretching structures is well developed. However, in spite of numerous studies, the geodynamic significance of this Cretaceous continental scale extension remains unclear (Fig. 17). Plate-boundary or intracrustal processes cannot satisfactorily explain all the geological features of this extension. The models involving lithosphere removal must be put forward to account for the destruction of the North China Craton. Asthenospheric convection or “erosion” of the

mantle lithosphere might account for craton thinning, crustal weakening and development of a tensional regime throughout a wide (> 1200 km) area of eastern Eurasian continent during late Mesozoic times. Nevertheless, in the present state of knowledge, additional geological, geochronological and geophysical investigations such as precise time span of the compression and extension events as well as the switching time from one regime to the other are needed to reach a satisfying understanding of the geodynamic significance of the continental-scale Mesozoic extension in the eastern part of the Eurasian continent.

Acknowledgments

Field and laboratory expenses have been supported by by Chinese National 973 Project (grant 2009CB825008) and NSFC (90714007, 40872142). Sincere thanks are presented to two reviewers and Guest Editor of this special issue for their constructive suggestions.

References

M.B. Allen, D.I. McDonald, X. Zhao, S. Vincent, C. Brouet-Menzies Early Cenozoic two-phase extension and late Cenozoic thermal subsidence and inversion of the Bohai Basin, Northern China Marine Petrology Geology, 14 (1997), pp. 951–972

B. Bryant, J. Ayers, S. Gao, C. Miller, H. Zhang Geochemical, age, and isotopic constraints on the location of the Sino-Korean/Yangtze Suture and evolution of the Northern Dabie Complex, east central China Geological Society of America Bulletin, 116 (2004), pp. 698–717 http://dx.doi.org/10.1130/B25302.1

R.W. Carlson, D.G. Pearson, D.E. James Physical, chemical, and chronological characteristics of continental mantle Reviews of Geophysics, 43 (2005) 2004RG000156

Charles, N., 2010. Mechanisms of Mesozoic continental extension in East Asia. Ph. D thesis, Orleans University, 1–475.

N. Charles, C. Gumiaux, R. Augier, Y. Chen, W. Lin, R. Zhu Metamorphic Core Complex vs. Synkinematic pluton in continental extension setting: insights from key structures (Shandong Province, eastern China) Journal of Asian Earth Sciences, 40 (2011), pp. 261–278 http://dx.doi.org/10.1016/j. jseaes. 2010. 07. 006

A. Chen Geometric and kinematic evolution of basement-cored structure: intraplate orogenesis within the Yanshan Orogen, North China Tectonophysics, 292 (1998), pp. 17–42

B. Chen, B.M. Jahn, W. Tian Evolution of the Solonker suture zone: constraints from zircon U–Pb ages, Hf isotopic ratios and whole-rock Nd–Sr isotope compositions of subduction- and collision-related magmas and forearc sediments Journal of Asian Earth Sciences, 34 (2008), pp. 245–257 http://dx.doi.org/10.1016/j.jseaes.2008.05.007

R.Y. Cheng, F.Y. Wu, W. Ge, D. Sun, X. Liu, J. Yang Emplacement age of the Raohe Complex in eastern Heilongjiang province and the tectonic evolution of the eastern part of Northeastern China Acta Petrologica Sinica, 22 (2006), pp. 315–325 (In Chinese with English abstract)

S.G. Choi, S.T. Kwon, J.H. Ree, C.S. So, S.J. Pak Origin of Mesozoic Gold mineralization in South Korea The Island Arc, 14 (2005), pp. 102–114

S.K. Chough, S.T. Kwon, J.H. Ree, D.K. Choi Tectonic and sedimentary evolution of the Korean Peninsula: a review and new view Earth-Science Reviews, 52 (2000), pp. 175–235

S. Cui, Z. Wu On the Mesozoic and Cenozoic intracontinental orogenesis of the Yanshan area, China ,in: Y. Zheng (Ed.), Proceedings of the 30th International Geological Congress, 14VSP, Utrecht, The Netherlands (1997), pp. 277–292

Y. Daoudene, D. Gapais, P. Ledru, A. Cocherie, S. Hocquet, T.V. Donskaya The Ereendavaa Range (north-eastern Mongolia): an additional argument for Mesozoic extension throughout eastern Asia International Journal of Earth Sciences, 98 (2009), pp. 1381–1393 http://dx.doi.org/10.1007/s00531-008-0412-2

Y. Daoudene, G. Ruffet, A. Cocherie, P. Ledru, D. Gapais Timing of exhumation of the Ereendavaa metamorphic core complex (north-eastern Mongolia)—U–Pb and $^{40}Ar/^{39}Ar$ constraints Journal of Asian Earth Sciences (2011)
http://dx.doi.org/10.1016/j.jseaes.2011.04.009

Darby, B.J., 2003. Mesozoic contractional deformation in the East Asian tectonic collage: the enigmatic northwest Ordos region, China. Ph.D. Dissertation, University of Southern California, Los Angeles, 1–174.

B.J. Darby, G.A. Davis, Y. Zheng Structure evolution of the southwestern Daqingshan, Yinshan belt, Inner Mongolia, China ,in: M.S. Hendrix, G.A. Davis (Eds.), Paleozoic and Mesozoic tectonic evolution of Central and Asia: From Continental Assembly to Intracontinental Deformation, Geological Society of American Memoir, 194 (2001), pp. 199–214

B.J. Darby, G.A. Davis, X. Zhang, F. Wu, S. Wilde, J. Yang The newly discovered Waziyu metamorphic core complex, Yiwulüshan, western Liaoning province, Northwest China Earth Science Frontiers, 11 (2004), pp. 145–155

G.A. Davis, B.J. Darby Early Cretaceous overprinting of the Mesozoic Daqing Shan fold-and-thrust belt by the Hohhot metamorphic core complex, Inner Mongolia, China Earth Science Frontiers, 17 (2010), pp. 1–20

G.A. Davis, X. Qian, Y. Zheng, H. Yu, C. Wang, T.H. Mao, G.E. Gehrels, S. Muhammad, J.E. Fryxell Mesozoic deformation and plutonism in the Yunmeng Shan: a Chinese metamorphic core complex north of Beijing, China A. Yin, T.A. Harrison (Eds.), The Tectonic Evolution of Asia, Cambridge University Press, New York (1996), pp. 253–280

G.A. Davis, C. Wang, Y. Zheng, J. Zhang, C. Zhang, G.E. Gehrels The enigmatic Yinshan fold-and-thrust belt of northern China: new views on its intraplate contractional styles Geology, 26 (1998), pp. 43–46

G.A. Davis, Y. Zheng, C. Wang, B.J. Darby, Ch. Zhang, G.E. Gehrels Mesozoic tectonic evolution of the Yanshan fold and thrust belt, with emphasis on Hebei and Liaoning provinces, northern China ,in: M.S. Hendrix, G.A. Davis (Eds.), Paleozoic and Mesozoic

tectonic evolution of Central and Asia: From Continental Assembly to Intracontinental Deformation, Geological Society of American Memoir, 194 (2001), pp. 171–194

G.A. Davis, B.J. Darby, Y. Zheng, T.L. Spell Geometric and temporal evolution of an extensional detachment fault, Hohhot metamorphic core complex, Inner Mongolia, China Geology, 30 (2002), pp. 1003–1006

G.A. Davis, B. Xu, Y.D. Zheng, W.J. Zhang Indosinian extension in the Solonker suture zone: the Sonid Zuoqi metamorphic core complex, Inner Mongolia, China Earth Science Frontiers, 11 (2004), pp. 135–143

G.A. Davis, J.F. Meng, W.R. Cao, X.Q. Du Triassic and Jurassic tectonics in the eastern Yanshan Belt, North China: insights from the controversial Dengzhangzi Formation and its neighboring units Earth Science Frontiers, 16 (2009), pp. 69–86

J. Deng, X. Mo, H. Zhao, Z. Wu, Z. Luo, S. Su A new model for the dynamic evolution of Chinese lithosphere: continental roots–plume tectonics Earth-Science Reviews, 65 (2004), pp. 223–275

H.G. Dill, S. Altangerel, J. Bulgamaa, O. Hongor, S. Khishigsuren, Y. Majigsuren, S. Myagmarsuren, C. Heunisch The Baganuur coal deposit, Mongolia: depositional environments and paleoecology of a Lower Cretaceous coal-bearing intermontane basin in Eastern Asia International Journal of Coal Geology, 60 (2004), pp. 197–236

T.V. Donskaya, B.F. Windley, A.M. Mazukabzov, A. Kröner, E.V. Sklyarov, D.P. Gladkochub, V.A. Ponomarchuk, G. Badarch, M.K. Reichow, E. Hegner Age and evolution of late Mesozoic metamorphic core complexes in southern Siberia and northern Mongolia Journal of the Geological Society of London, 165 (2008), pp. 405–421

J. Du, Y. Ma, Y. Zhao, Y. Wang SHRIMP U–Pb zircon dating of the Yiwulüshan granite in western Liaoning and its geological implications Geology in China, 24 (2007), pp. 26–33

B.O. Erdenetsogt, I. Lee, D. Bat-Erdene, L. Jargal Mongolian coal-bearing basins: geological settings, coal characteristics, distribution, and resources International Journal of Coal Geology, 80 (2009), pp. 87–104

A. Etchecopar Kinematic model of progressive deformation in polycrystalline aggregate Tectonophysics, 39 (1977), pp. 121–139

M. Faure, Y. Sun, L. Shu, P. Monié, J. Charvet Extensional tectonics within a subduction-type orogen. The case study of the Wugongshan dome (Jiangxi Province, SE China) Tectonophysics, 263 (1996), pp. 77–108

M. Faure, W. Lin, L. Shu, Y. Sun, U. Schärer Tectonics of the Dabieshan (E. China) and possible exhumation mechanism of ultra high-pressure rocks Terra Nova, 11 (1999), pp. 251–258

M. Faure, W. Lin, U. Schärer, L. Shu, Y. Sun, N. Arnaud Continental subduction and exhumation of UHP rocks. Structural and geochronological insights from the Dabieshan (E. China) Lithos, 70 (2003), pp. 213–241

M. Faure, P. Trap, W. Lin, P. Monié, O. Bruguier Polyorogenic evolution of the Paleoproterozoic Trans-North China Belt, new insights from the in Lüliangshan–Hengshan–Wutaishan and Fuping massifs Episodes, 30 (2007), pp. 96–107

S. Gao, R.L. Rudnick, R.W. Carlsonet, W.F. McDonough, Y.S. Liu Re–Os evidence for replacement of ancient mantle lithosphere beneath the North China Craton Earth and Planetary Science Letters, 198 (2002), pp. 307–322

S.A. Graham, M.S. Hendrix, C.L. Johnson, D. Badamgarav, G. Badarch, J. Amory, M. Porter, R. Barsbold, L.E. Webb, B.R. Hacker Sedimentary record and tectonic implications of Mesozoic rifting in southeast Mongolia Geological Society of America Bulletin, 113 (2001), pp. 1560–1579

H. Guan, J. Liu, M. Ji Discovery of the Wanfu metamorphic core complex in southern Liaoning and its regional tectonic implication Earth Science Frontiers, 15 (2008), pp. 199–208 (In Chinese with English abstract)

B.R. Hacker, S.R. Wallis, L. Ratschbacher, M. Grove, G. Gehrels High-temperature geochronology constraints on the tectonic history and architecture of the ultrahigh-pressure Dabie–Sulu orogeny Tectonics, 25 (2006), p. TC5006 http://dx.doi.org/10.1029/2001JB001129/2005TC001937

B.R. Hacker, S.R. Wallis, M.O. McWilliams, P.B. Gans $^{40}Ar/^{39}Ar$ constraints on the tectonic history and architecture of the ultrahigh-pressure Sulu orogeny Journal of Metamorphic Geology, 27 (2009), pp. 1–18 http://dx.doi.org/10.1111/j.1525-1314.2009.00840.x

B. Han, Y. Zheng, J. Gan, Z.H. Chang The Luozidian normal fault near Chifeng, Inner Mongolia: master fault of a quasi-metamorphic core complex International Geology Review, 43 (2001), pp. 254–264

HBGMR, Hebei Bureau of Geology and Mineral Resources Regional geology of Hebei Province: Ministry of Geology and Mineral Resources, Geological Memoirs, ser. 1, no. 15 (1989) 1741 pp. (in Chinese with English summary)

Z.J. He, J.Y. Li, B.G. Niu, J.S. Ren A Late Jurassic intense thrusting-uplifting event in the Yanshan–Yinshan area, northern China, and its sedimentary response Geological Review, 44 (1998), pp. 407–418

J. Hu, Y. Zhao, W. Liu, G. Xu Early Mesozoic deformations of the eastern Yanshan thrust belt, northern China International Journal of Earth Sciences, 99 (2010), pp. 785–800 http://dx.doi.org/10.1007/s00531-009-0417-5

J.L. Huang, D.P. Zhao High-resolution mantle tomography of China and surrounding regions Journal of Geophysical Research, 111 (2006) 2005JB004066

W. Ji, W. Lin, Y. Shi, Q. Wang, Y. Chu Structure and evolution of the Early Cretaceous Dabieshan metamorphic core complex Chinese Journal of Geology, 46 (2011), pp. 161–180

G.L. Kirillova Late Mesozoic–Cenozoic sedimentary basins of active continental margin of Southeast Russia: paleogeography, tectonics, and coal–oil–gas presence Marine and Petroleum Geology, 20 (2003), pp. 385–397

T.M. Kusky Geophysical and geological tests of tectonic models of the North China Craton Gondwana Research, 20 (2011), pp. 26–35

T.M. Kusky, J.H. Li Paleoproterozoic tectonic evolution of the North China Craton Journal of Asian Earth Sciences, 22 (2003), pp. 383–397

R.D. Law Crystallographic fabrics: a selective review of their applications to research in structural geology ,in: R.J. Knipe, E.H. Rutter (Eds.), Deformation Mechanisms, Rheology and Tectonics, Geological Society of London, Special Publications, 54 (1990), pp. 335–352

LBGMR, Liaoning Bureau of Geology and Mineral Resources Regional Geology of Liaoning Province, Geol. Mem., Ser.1, 14Geol. Publ. House (1989), pp. 1–856 (in Chinese with English summary)

D.W. Lee Strike-slip fault tectonics and basin formation during the Cretaceous in the Korean Peninsula The Island Arc, 8 (1999), pp. 218–231

S. Li Analysis of Extensional Basin and its Fashion, Geol. Publ. House (1994), pp. 1–125 (in Chinese with English summary)

X.H. Li Cretaceous magmatism and lithospheric extension in southeast China Journal of Asian Earth Sciences, 18 (2000), pp. 293–305

S. Li, F. Lu, Ch. Lin Evolution of Mesozoic and Cenozoic basins in Eastern China and their Geodynamic Background, China University of Geosciences Press, Wuhan (1997), pp. 1–239 In Chinese with English summary

S. Li, G. Zhao, L. Dai, L. Zhou, X. Liu, Y. Suo, M. Santosh Cenozoic faulting of the Bohai Bay Basin and its bearings on the destruction of the eastern North China Craton Journal of Asian Earth Sciences (2011) http://dx.doi.org/10.1016/j.jseaes.2011.06.011

S. Li, G. Zhao, L. Dai, X. Liu, L. Zhou, M. Santosh, Y. Suo Mesozoic Basins in eastern China and their Bearings on the deconstruction of the North China Craton Journal of Asian Earth Sciences (2011) http://dx.doi.org/10.1016/j.jseaes.2011.06.008

W. Lin, Q. Wang Late Mesozoic extensional tectonics in North China Block—response to the Lithosphere removal of North China Craton? Bulletin de la Société Géologique de France, 177 (2006), pp. 287–294

W. Lin, M. Faure, P. Monié, U. Schärer, L. Zhang, Y. Sun Tectonics of SE China, new insights from the Lushan massif (Jangxi Province) Tectonics, 19 (2000), pp. 852–871

W. Lin, M. Faure, P. Monié, Q.C. Wang Polyphase Mesozoic tectonics in the eastern part of the North China Blocks: insights from the Liaoning Peninsula massif (NE China) ,in: M.G. Zhai, B.F. Windley, T.M. Kusky, Q.R. Meng (Eds.), Mesozoic sub-continental lithospheric thinning under eastern Asia, Geological Society, London, Special Publications, 280 (2007), pp. 153–170

W. Lin, M. Faure, P. Monié, U. Schärer, D. Panis Mesozoic extensional tectonics in Eastern Asia: the South Liaodong Peninsula Metamorphic Core Complex (NE China) Journal of Geology, 116 (2008), pp. 134–154

W. Lin, Q.C. Wang, J. Wang, F. Wang, Y. Chu, K. Chen Late Mesozoic extensional tectonics of the Liaodong Peninsula massif: response of crust to continental lithosphere destruction of the North China Craton Science China Earth Sciences, 54 (2011), pp. 843–857 http://dx.doi.org/10.1007/s11430-011-4190-5

Lin, W., Faure, M., Chen, Y., Ji, W., Wang, F., Wu, L., Charles, N., Wang, Q. this issue. Late Mesozoic compressional to extensional deformations in Yiwulüshan massif, NE China and their bearing on Yinshan–Yanshan orogenic belt (Part II: Anisotropy of magnetic susceptibility and gravity modeling). Gondwana Research.

G.S. Lister, G.A. Davis The origin of metamorphic core complexes and detachment faults formed during Tertiary continental extension in the northern Colorado River region, U.S.A Journal of Structural Geology, 11 (1989), pp. 65–94

J. Liu, X. Liu, S. Si, G. Li, Z. Ouyang Characterics and genesis of granitic complex in Fuxing–Jinzhou area, Liaoning province Geology and Geochemistry, 28 (2000), pp. 65–74

Z. Liu, Z. Xu, Z. Yang Mesozoic crustal overthrusting and extensional deformation in the Yinshan Mountains area Geological Bulletin of China, 21 (2002), pp. 246–250

J. Liu, G. Davis, Z. Lin, F. Wu The Liaonan metamorphic core complex, southeastern Liaoning Province, North China: a likely contributor to Cretaceous rotation of eastern Liaoning, Korea and contiguous areas Tectonophysics, 407 (2005), pp. 65–80

LNBGMR-Yixian, 1970. Bureau of Geological and Mineral Resources of Liaoning Province, Geological Map of Yixian, Scale 1:200 000. China Ministry of Geology and Mineral Resource, Beijing.

J. Lü, W. Liu Features of Indosian structures in Kalafangzi area Liaoning Geology, 12 (1994), pp. 255–262

Y. Ma, S. Cui, G. Wu, Z. Wu, D. Zhu, X. Li, X. Feng The structural feature of metamorphic core complex in Yiwulüshan Mountains, West Liaoning Acta Geoscientia Sinica, 20 (1999), pp. 385–391 in Chinese

Y. Ma, S. Cui, G. Wu, Z. Wu, D. Zhu, X. Li, X. Feng Uplift history of the Yiwulüshan mountains in west Liaoning Acta Geoscientia Sinica, 21 (2000), pp. 245–253 (in Chinese)

M. Mattauer, P. Matte, J. Malavieille, P. Tapponnier, H. Maluski, Z. Xu, Y. Lu, Y. Tang Tectonics of Qinling belt: build-up and evolution of eastern Asia Nature, 317 (1985), pp. 496–500

A.M. Mazukabzov, T.V. Donskaya, D.P. Gladkochub, E.V. Sklyarov, V.A. Ponomarchuk, E.B. Sal'nikova Structure and age of the metamorphic core complex of the Burgutui ridge (Southwestern Transbaikal region) Doklady Earth Sciences, 407 (2006), pp. 179–183

Q. Meng What drove late Mesozoic extension of the northern China–Mongolia tract? Tectonophysics, 369 (2003), pp. 155–174

Q. Meng, J. Hu, J. Jin, Y. Zhang, D. Xu Tectonics of the late Mesozoic wide extension basin system in the China–Mongolia border region Basin Research, 15 (2003), pp. 397–415

D.V. Metelkin, V.A. Vernikovsky, A.Y. Kazansky, M.T.D. Wingate Late Mesozoic tectonics of Central Asia based on paleomagnetic evidence Gondwana Research, 18 (2010), pp. 400–419

C.W. Passchier, R.A.J. Trouw Microtectonics, 48Springer (1996), pp. 257–260

Y. Peng, L. Zhang, W. Chen, C. Zhang, S. Guo, D. Xing, B. Jia, S. Chen, Q. Ding $^{40}Ar/^{39}Ar$ and K–Ar dating of the Yixian Formation volcanic rocks, Western Liaoning province, China Geochimica, 32 (2003), pp. 427–435

L. Ratschbacher, B.R. Hacker, L. Webb, M.O. McWilliams, T. Ireland, S. Dong, A. Calvert, D. Chateigner, H. Wenk Exhumation of ultrahigh-pressure continental crust in east central China: Cretaceous and Cenozoic unroofing and the Tan-Lu fault Journal of Geophysical Research, 105 (2000), pp. 13303–13338

L. Ratschbacher, B.R. Hacker, A. Calvert, L. Webb, J.C. Grimmer, M.O. McWilliams, T. Ireland, S. Dong, J. Hu Tectonics of the Qinling (Central China): tectonostratigraphy, geochronology, and deformation history Tectonophysics, 366 (2003), pp. 1–53

J. Ren, K. Tamaki, S. Li, Z. Junxia Late Mesozoic and Cenozoic rifting and its dynamic setting in Eastern China and adjacent areas Tectonophysics, 344 (2002), pp. 175–205

J.C. Schmid, L. Ratschbacher, B.R. Hacker, I. Gaitzsch, S. Dong How did the foreland react? Yangtze foreland fold and thrust belt deformation related to exhumation of the Dabie Shan ultrahigh-pressure continental crust (eastern China) Terra Nova, 11 (1999), pp. 266–272

A.M.C. Sengor, B.A. Natal'in Paleotectonics of Asia: fragments of a synthesis A. Yin, T.A. Harrison (Eds.), The Tectonic Evolution of Asia, Cambridge University Press, New York (1996), pp. 486–641

Q. Shang Occurrences of Permian radiolarians in central and eastern Nei Mongol (Inner Mongolia) and their geological significance to the Northern China Orogen Chinese Sciences Bulletin, 49 (2004), pp. 2613–2619

J.E. Spencer Role of tectonic denudation in warping and uplift of low angle normal faults Geology, 12 (1984), pp. 95–98

P. Trap, M. Faure, W. Lin, P. Monié Late Palaeoproterozoic (1900–1800 Ma) nappe stacking and polyphase deformation in the Hengshan–Wutaishan area: implication for the understanding of the Trans-North China Belt, North China Craton Precambrian Research, 156 (2007), pp. 85–106

J.J. Traynor, C. Sladen Tectonic and stratigraphic evolution of the Mongolian People's Republic and its influence on hydrocarbon geology and potential Marine and Petroleum Geology, 12 (1995), pp. 35–52

S. Turner, N. Arnaud, J. Liu, N. Rogers, C. Hawkesworth, N. Harris, S. Kelley, P. van Calsteren, W. Deng Post-collision, shoshonitic volcanism on the Tibetan Plateau implications for convective thinning of the lithosphere and the source of ocean island basalts Journal of Petrology, 37 (1996), pp. 45–71

Q. Wang, X. Liu Paleoplate tectonics between Cathaysia and Angaraland in Inner Mongolia of China Tectonics, 5 (1986), pp. 1073–1088

L.G. Wang, Y.M. Qiu, N.J. McNaughton, D.I. Groves, Z.K. Luo, J.Z. Huang, L.C. Miao, Y.K. Liu Constraints on crustal evolution and gold metallogeny in the Northwestern Jiaodong Peninsula, China, from SHRIMP U–Pb zircon studies of granitoids Ore Geology Reviews, 13 (1998), pp. 275–291

W. Wang, S. Lu, Y. Guo, Y. Sun Tectonic geometry and type of traps in Fuxin Basin ournal of the University of Petroleum, 22 (1998), pp. 26–30

P.J. Wang, Z.J. Liu, S.X. Wang, W.H. Song $^{40}Ar/^{39}Ar$ and K/Ar dating on the volcanic rocks in the Songliao basin, NE China: constraints on stratigraphy and basin dynamics International Journal of Earth Sciences, 91 (2002), pp. 331–340

F. Wang, X.H. Zhou, L.C. Zhang, J.F. Ying, Y.T. Zhang, F.Y. Wu, R.X. Zhu Late Mesozoic volcanism in the Great Xing'an Range (NE China): timing and implications for the dynamic setting of NE Asia Earth and Planetary Science Letters, 251 (2006), pp. 179–198

J. Wang, M. Faure, Y. Chen, W. Lin Polyphase deformation recorded from Mesozoic granitoids in the North China Block and its geodynamic significance, example from the Yunmengshan granodiorite, 13European Geosciences Union, Vienna (2011) EGU2011-1798

T. Wang, Y. Zheng, J. Zhang, L. Zeng, T. Donskaya, L. Guo, J. Li Pattern and kinematic polarity of late Mesozoic extension in continental NE Asia: perspectives from metamorphic core complexes Tectonics (2011) http://dx.doi.org/10.1029/2011TC002896

Y. Wang, L. Zhou, J. Li Intracontinental superimposed tectonics—a case study in the Western Hills of Beijing, eastern China Geological Society of America Bulletin, 123 (2011), pp. 1033–1055 http://dx.doi.org/10.1130/B30257.1

M.P. Watson, A.B. Hayward, D.N. Parkinson, Z.M. Zhang Plate tectonic history, basin development and petroleum source rock deposition onshore China Marine and Petroleum Geology, 4 (1987), pp. 205–225

L.E. Webb, S.A. Graham, C.L. Johnson, G. Badarch, S. Hendrix Occurrence, age, and implications of the Yagan–Onch Hayrhan metamorphic core complex, southern Mongolia Geology, 27 (1999), pp. 143–146

B. Wernicke Cenozoic extensional tectonics of the U.S. Cordillera ,in: B.C. Burchfiel, P.W. Lipman, M.L. Zoback (Eds.), The Geology of North America, G3, The Cordillera orogen: conterminous US, Geological Society Of America, United States (1992), pp. 553–581

W.H. Wong The Mesozoic orogenic movement in eastern China Bulletin of the Geological Society of China, 8 (1929), pp. 33–44

J. Wong, M. Sun, G. Xing, X.H. Li, G. Zhao, K. Wong, C. Yuan, W. Xia, L. Li, F.Y. Wu Geochemical and zircon U–Pb and Hf isotopic study of the Baijuhuajian metaluminous A-type granite: extension at 125–100 Ma and its tectonic significance for South China Lithos, 112 (2009), pp. 289–305

F.Y. Wu, B.M. Jahn, S. Wilde, D.Y. Sun Phanerozoic crustal growth: U–Pb and Sr–Nd isotopic evidence from the granites in northeastern China Tectonophysics, 328 (2000), pp. 89–113

F.Y. Wu, J.Q. Lin, S.A. Wilde, D.Y. Sun, J.H. Yang Nature and significance of the Early Cretaceous giant igneous event in eastern China Earth and Planetary Science Letters, 233 (2005), pp. 103–119

F.Y. Wu, J.H. Yang, S.A. Wilde, X.O. Zhang Geochronology, petrogenesis and tectonic implications of Jurassic granites in the Liaodong Peninsula, NE China Chemical Geology, 221 (2005), pp. 127–156

F.Y. Wu, J. Yang, Y. Zhang, X. Liu Emplacement ages of the Mesozoic granites in southeastern part of the Western Liaoning Province Acta Petrologica Sinica, 22 (2006), pp. 315–325

F.Y. Wu, R.H. Han, J.H. Yang, S.A. Wilde, M.G. Zhai, S.C. Park Initial constraintson the timing of granitic magmatism in North Korea using U–Pb zircon geochronology Chemical Geology, 238 (2007), pp. 232–248

F.Y. Wu, Y.G. Xu, S. Gao, Y. Zheng Lithospheric thinning and destruction of the North China Craton Acta Petrologica Sinica, 24 (2008), pp. 1145–1174 (In Chinese with English abstract)

W. Xiao, B.F. Windley, J. Hao, M. Zhai Accretion leading to collision and the Permian Solonker suture, Inner Mongolia, China: termination of the Central Asian orogenic belt Tectonics, 22 (2003) http://dx.doi.org/10.1029/2002TC001484

B. Xu, B. Chen Framework and evolution of the middle Paleozoic oroginic belt between Siberian and North China Plates in northern Inner Mongolia Science in China Series D, 40 (1997), pp. 463–469

Z.C. Xu, Z.M. Wang Geotectonic features of Yanshan area in Hebei province Regional Geology of China, 3 (1983), pp. 39–55 (in Chinese with English abstract)

J. Yang, F.Y. Wu Triassic magmatism and its relation to decrationization in the eastern North China Craton Science China Earth Sciences, 52 (2009), pp. 1319–1330 http://dx.doi.org/10.1007/s11430-009-0137-5

G. Yang, Y. Chai, Z. Wu Thin-skinned thrust nappe structures in western Liaoning in the Eastern Sector of the Yanshan orogenic belt Acta Geologica Sinica, 75 (2001), pp. 322–332

J.H. Yang, S.L. Chung, S.A. Wilde, F.Y. Wu, M. Chu, Ch. Lo, H. Fan Petrogenesis of post orogenic syenites in the Sulu Orogenic Belt, East China: geochronology, geochemical and Nd–Sr isotopic evidence Chemical Geology, 214 (2005), pp. 99–125

J.H. Yang, F.Y. Wu, J.A. Shao, L. Xie, X. Liu In-situ U–Pb dating and Hf Isotopic analyses of zircon from volcanic rockss of the Houcheng and Zhang jiakou formations in the Zhang–Xuan Area, Northeast China Earth Science—Journal of China University of Geosciences, 31 (2006), pp. 71–80 (In Chinese with English abstract)

J.H. Yang, F.Y. Wu, S.L. Chung, Ch.H. Lo The extensional geodynamic setting of Early Cretaceous granitic intrusions in the eastern North China Craton: evidence from laser ablation $^{40}Ar/^{39}Ar$ dating of K-bearing minerals Acta Petrologica Sinica, 24 (2008), pp. 1175–1184 (In Chinese with English abstract)

Yin, G., 2007. The tectonic features and the establishment's FEM simulation of metamorphic core complex in Yiwulv Mountains. M. D. Dissertation, Jinlin University, Changchun. 48pp.

A. Yin, S. Nie An Indentation model for the North and South China collision and the development of the Tan-lu and normal fault systems, Eastern Asia Tectonics, 12 (1993), pp. 801–813

A. Yin, S. Nie A Phanerozoic palinspastic reconstruction of China and its neighboring regions A. Yin, T.A. Harrison (Eds.), The Tectonic Evolution of Asia, Cambridge University Press, New York (1996), pp. 442–485

M.G. Zhai, M. Santosh The early Precambrian odyssey of the North China Craton: a synoptic overview Gondwana Research, 20 (2011), pp. 6–25

M. Zhai, R. Zhu, J. Liu, Q. Meng, Q. Hou, S. Hu, W. Liu, Zh. Li, H. Zhang Time range of Mesozoic tectonic regime inversion in eastern North China Block Science China Earth Sciences, 47 (2004), pp. 151–159

H.F. Zhang, M. Sun Geochemistry of Mesozoic basalts and mafic dikes in southeastern North China craton, and tectonic implication International Geology Review, 44 (2002), pp. 370–382

J.J. Zhang, Y. Zheng, Q. Shi, X. Yu, Q. Zhang The Xiaoqinling detachment fault and metamorphic core complex of China: structure, kinematics, strain and evolution Proc. 30th. International Geological Congress, 14 (1997), pp. 158–172

X. Zhang, Q. Yu, F. Chen, X. Wang Strucutral characters, origin and evolution of metamorphic core complex in Central basement uplift and Xujiaweizi faulted depression in Songliao basin, Northeast China Earth Science Frontiers, 7 (2000), pp. 411–419

H.F. Zhang, Z.Q. Zhong, S. Gao, B. Zhang, H. Li U–Pb zircon age of the foliated garnet-bearing granites in western Dabie Mountains, Central China Chinese Science Bulletin, 46 (2001), pp. 1657–1660

X. Zhang, T. Li, Z. Pu $^{40}Ar/^{39}Ar$ thermochronology of two ductile shear zones from YiwulüShan, west Liaoning region: age constraints on Mesozoic tectonic events Chinese Science Bulletin, 47 (2002), pp. 697–701

L.C. Zhang, Y.C. Shen, T.B. Liu, Q.D. Zeng, G.M. Li, H.M. Li $^{40}Ar/^{39}Ar$ and Rb–Sr isochron dating of the gold deposits on northern margin of the Jiaolai Basin, Shandong, China Science in China Series D, 46 (2003), pp. 708–718

H. Zhang, W. Wang, Z. Li, F. Yang, L. Zhang, S. Zheng Study of two period ductile deformations in Yiwulüshan area of western Liaoning in Mesozoic Global Geology, 23 (2004), pp. 213–219

H. Zhang, H. Yuan, Z. Hu, X. Liu, C. Diwu U–Pb zircon dating of the Mesozoic Volcanic Strata in Luanping of North Hebei and its significance Earth Science—Journal of China University of Geosciences, 30 (2005), pp. 707–720

X. Zhang, Q. Miao, H. Zhang, S. Wilde A Jurassic peraluminous leucogranite from Yiwulüshan, western Liaoning, North China craton: age, origin and tectonic significance Geological Magazine, 145 (2008), pp. 305–320

C.H. Zhang, C.M. Li, H.L. Deng, Y. Liu, L. Liu, B. Wei, H.B. Li, Z. Liu Mesozoic contraction deformation in the Yanshan and northern Taihang mountains and its implications to the destruction of the North China Craton Science China Earth Sciences, 54 (2011), pp. 798–822

Y. Zhao The Mesozoic orogenics and tectonic evolution of the Yanshan Area Geological Review, 36 (1990), pp. 1–13 (in Chinese with English abstract)

L. Zhao, M. Xue Mantle flow pattern and geodynamic cause of the North China Craton reactivation: evidence from seismic anisotropy Geochemistry, Geophysics, Geosystems, 11 (2010), p. Q07010 http://dx.doi.org/10.1029/2010GC003068

G. Zhao, M. Sun, S.A. Wilde, S. Li Assembly, accretion and breakup of the Paleo-Mesoproterozoic Columbia Supercontinent: records in the North China Craton Gondwana Research, 6 (2003), pp. 417–434

Y. Zhao, G. Xu, S. Zhang, Z. Yang, Y. Zhang, J. Hu Yanshanian movement and conversion of tectonic regimes in Eastern Asia Earth Science Frontiers, 11 (2004), pp. 319–328

Y. Zheng, S. Wang, Y. Wang An enormous thrust nappe and extensional metamorphic core complex newly discovered in Sino-Mongolian boundary area Science in China. Series B, 34 (1991), pp. 1145–1152

X.M. Zhou, W.X. Li Origin of Late Mesozoic igneous rocks in southeastern China: implications for lithospheric subduction and underplating of mafic magmas Tectonophysics, 326 (2000), pp. 269–287

X. Zhou, T. Sun, W. Shen, L. Shu, Y. Niu Petrogenesis of Mesozoic granitoids and volcanic rocks in South China: a response to tectonic evolution Episodes, 29 (2006), pp. 26–33

D. Zhu, X. Meng, X. Feng, Z. Shao, W. Qu, H. Zhang, H. Fu, J. Wang, M. Yang Tectonic features of metamorphic core complexes in Yiwulüshan area, Liaoning province and a dynamic analysis of rock fabrics Acta Geoscientia Sinica, 24 (2003), pp. 225–230 (in Chinese)

G. Zhu, C. Xie, W. Chen, B. Xiang, Z. Hu Evolution of the Hongzhen metamorphic core complex: evidence for Early Cretaceous extension in the eastern Yangtze craton, eastern China Geological Society of America Bulletin, 122 (2010), pp. 506–516

G. Zhu, D. Jiang, B. Zhang, Y. Chen Destruction of the eastern North China Craton in a backarc setting: evidence from crustal deformation kinematics Gondwana Research (2011) http://dx.doi.org/10.1016/j.gr.2011.08.005

R. Zhu, L. Chen, F. Wu, J. Liu Timing, scale and mechanism of the destruction of the North China Craton Science China Earth Sciences, 54 (2011), pp. 789–797

Y.A. Zorin Geodynamics of the western part of the Mongolia–Okhotsk collisional belt, Trans-Baikal region (Russia) and Mongolia Tectonophysics, 306 (1999), pp. 33–56